University of Alberta

Investigation of the neuroprotective effect of Phenelzine

by

Yoko Azumaya 

A thesis submitted to the Faculty of Graduate Studies and Research in partial fulfillment of the requirements for the degree of Master of Science

in

Neurochemistry

of

Department Psychiatry

Edmonton, Alberta

Fall 2004

Your file Votre référence
ISBN: 0-612-95704-7
Our file Notre référence
ISBN: 0-612-95704-7

Acknowledgements

I would like to sincerely thank my supervisor Dr. K.G. Todd for providing me with the ideal environment to conduct research and for constant and excellent supervision. I would like to express my gratitude to Drs. G.B. Baker and J-M. Le Melledo for their advice and comments as members of my committee. I would also like to extend my gratitude to Dr. S.M.J. Dunn for taking the time to serve as an examiner for my thesis defense.

I deeply appreciate Drs. V. Tanay and A. Holt, and G. Rauw for their help in my research. Without their excellent and patient assistance, some experiments performed in this thesis would have been extremely difficult or simply impossible for me to perform. They were also extremely helpful in proofreading my thesis. In that context especially, Dr. V. Tanay spent great deal of time correcting my thesis and for that I cannot express how truly grateful I am.

To my fellow students, especially L. Jantzie and B. Sowa, for making my everyday research so enjoyable. I also would like to thank J. van Muyden and P. Wolfaardt for making all the administrative procedures run smoothly so that I could focus on research.

I would like to thank Dr. D. Schubert (Salk Institute for Biological Studies, La Jolla, CA) for generously providing me with HT-22 cells. I also extend my gratitude to CIHR, Heart and Stroke Foundation of Canada, and the Davey Endowment for Brain Research for providing us funds to perform this research.

Table of contents

List of Figures

List of Tables

List of Abbreviations

AET	2-amino ethylisothiouronium bromide
AMPA	α-amino-3-hydroxy-5-methyl-4-isoxasole
ATP	adenosine triphosphate
BSA	bovine serum albumin
BSO	buthionine-[*S,R*]-sulfoximine
C. elegans	Caenorhabditis elegans
CNS	central nervous system
ddH_2O	double distilled H_2O
DMEM	Dulbecco's modified Eagles medium
DMSO	dimethyl sulfoxide
DTNB	5,5'-dithiobis-2-nitrobenzoic acid (Ellman's reagent)
EAAT	excitatory amino acid transporter
FBS	fetal bovine serum
G-6-P	glucose-6-phosphate
G-6-P-DH	glucose-6-phosphate dehydrogenase
GABA	γ-aminobutyric acid
GABA-T	GABA-transaminase
GAD	glutamic acid decarboxylase
GC	gas chromatography
GGT	γ-glutamyltranspeptidase
Glu	glutamate
GR	glutathione reductase
GSH	glutathione

HBSS	Hank's balanced salt solution
HPLC	high performance liquid chromatography
ICC	immunocytochemistry
MAOI	monoamine oxidase inhibitor
MAP2	microtubule associated protein 2
MCA	middle cerebral artery
MTT	3-(4,5-dimethyldiazol-2-yl)-2,5-diphenyltetrazolium bromide
NAD	β-nicotinamide adenine dinucleotide
NADP	NAD-3'-phosphate
NAP	N^2-acetylphenelzine
NHS	normal horse serum
NMDA	N-methyl-D-asparate
OPA	*o*-phthaldialdehyde
PB	phosphate buffer
PBS	phosphate buffered solution
PEH	β-phenylethylidenehydrazine
PLP	pyridoxal-5'-phosphate
PLZ	phenelzine
ROS	reactive oxygen species
RT	reverse transcription
SDS	sodium dodecyl sulfate
SDS-PAGE	SDS-polyacrylamide gel electrophoresis
TBS	Tris buffered saline
THCl	Triton X100-HCl solution

THF	tetrahydrofuran
TNB	5-thiobis-2-nitrobenzoate
TNF	tumor necrosis factor
TOA	tri-n-octylamine
TTBS	0.1% Tween 20 in TBS
TTBS-milk	5% (w/v) skim milk powder in TTBS

Chapter 1 General Introduction

1.1 Neuronal degeneration in ischemia and neuronal diseases

Cerebral ischemia (stroke) is the fourth leading cause of death in Canada (Heart and Stroke Foundation of Canada, 2002) and survivors suffer from a variety of physiological sequelae such as paralysis/paresis, neglect, loss of sense of touch and/or temperature, and loss of speech ability. Cerebral ischemia is defined as a reduction of the blood supply to the central nervous system (CNS). There are two main types of cerebral ischemia, referred to as focal and global ischemia. Focal ischemia is the predominant pathology among patients and a thromboembolic occlusion of an artery is the most common cause (Moody et al., 2003). Thromboembolic occlusion occurs when a fragment of atherosclerotic plaque occludes cerebral blood vessels. Global cerebral ischemia is less common and the main causes are a complete stop of the blood supply to the brain due to cardiac arrest, no oxygen supply due to near drowning, or carbon monoxide poisoning (Cheung, 2003). Normally, the resting human brain receives approximately 55 ml/100 g/min of blood. A reduction in cerebral blood flow (CBF) to 15-20% below normal levels leads to an irreversible acute cell death, termed necrosis. A reduction in blood flow to 25-50% of normal CBF can cause delayed cell death, termed apoptosis (Schroder et al., 1996). However, a reduction in CBF by less than 50% if not prolonged, can be generally compensated for and does not lead to major physiological disturbance.

1.2 Necrosis and Apoptosis

According to Kerr et al. (1972), apoptosis was originally differentiated from necrosis by a distinct morphology. Necrosis is characterized by cell swelling and ultimately, bursting. The spillage of the intracellular contents causes an inflammatory response in the surrounding tissue. Apoptosis on the other hand, is characterized by shrinkage of the cell accompanied by nuclear changes including chromatin condensation, ultimately leading to cell fragmentation into membrane-bound apoptotic bodies. Typically, in apoptosis, there is observable morphological change to intracellular organelles such as the mitochondria. The fragmented cells are then phagocytosed by the brain's microglia cells. Apoptotic cells also display a nuclear DNA fragmentation at every 180 base pairs (Bortner et al., 1995), an upregulation and activation of a series of proteins (Ashe and Berry, 2003) including proteases (caspases; Kumar, 1995), tumor necrosis factor (TNF; Hasegawa and Bonavida, 1989) and the bcl protooncogene family (Merry and Korsmeyer, 1997).

Interestingly, in the mouse hippocampal neuronal cell derived cell line HT-22, the cell death induced by ischemic conditions results in the characteristics of both necrosis and apoptosis (Tan et al., 1998). In these cells, the DNA fragmentation consistent with apoptosis is not observed; yet they present some apoptotic characteristics such as activation of caspases (Amoroso, Gioielli et al. 1999), cell membrane shrinkage, and new protein synthesis (Tan et al., 1998).

1.2.1 Apoptotic factors – Bcl family

In *Caenorhabditis elegans* (*C. elegans*), 131 cells of the total 1090 cells the worm possesses die from apoptosis during development (Sulston, 2003). Fourteen genes have been shown to be involved in this apoptotic death pathway {see review by Liu and Hengartner (1999)}. Three of these genes, ced-3, ced-4 and ced-9, encode proteins responsible for the final step of apoptosis. The activation of ced-3 and -4 is required for cell death, but the activation of ced-9 can over-ride the program and cause the cell to survive. The inactivation of ced-3 or -4 by mutation results in the survival of all 131 cells that are normally destined to die through apoptosis. In contrast, the deletion of ced-9 function by mutation causes the 131, and other cells, to undergo apoptosis, leading to the death of the organism at an early point of development (Hengartner and Horvitz, 1994b). Results of the double mutation of ced-3 or ced-4 with that of ced-9 suggested that ced-9 inhibits the activity of ced-4 by binding to it (Ottilie et al., 1997) and this ced-9/ced-4 complex inhibits the activity of ced-3 (Wu et al., 1997). Homologues of the *C. elegans* genes are found in mammalian cells. The ced-3 gene is analogous to caspase 3 which is the final effector protein of apoptosis in mammalian cells (Xue et al., 1996). The ced-4 gene is analogous to mammalian apoptosis protease activating factor-1 (Apaf-1, Zou et al., 1997) and ced-9 is analogous to mammalian Bcl-2 (Hengartner and Horvitz, 1994a).

Bcl-2 belongs to the Bcl protein family. The Bcl protein family is interesting because it consists of both anti- and pro-apoptotic regulators. The family members Bcl-2 and Bcl-xL are the major anti-apoptotic factors and they can

inhibit cell death induced by a variety of factors. For example, overexpression of Bcl-xL in yeast protected cells from oxidative stress induced by H_2O_2 (Chen et al., 2003). Overexpression of Bcl-xL also protected a mammalian cell line, F:5.12 murine cells, from toxicity caused by induced accumulation of reactive oxygen species (Bojes et al., 1997). Both Bcl-2 and Bcl-xL have hydrophobic anchor sequences at the C-terminus that allows them to attach to the outer membrane of the mitochondria (Nguyen et al., 1993). Expression of truncated forms of either Bcl-2 or Bcl-xL protein that inhibited localization of the protein onto the mitochondria membrane reduced the protective properties of the proteins, suggesting that this is their site of action (Nguyen et al., 1994; Priault et al., 1999).

1.3 Effects of cerebral ischemia on brain glutamate levels

1.3.1 Extracellular accumulation of glutamate in ischemia

Glutamate (Glu) is the main excitatory neurotransmitter in the central nervous system and it plays important roles in many functions, including learning, memory and development. Excitatory neurotransmission is both oxygen- and glucose-dependent.

The mitochondria produce the majority of the cellular adenosine triphosphate (ATP) from glucose metabolism through oxidative phosphorylation using oxygen (Alberts et al., 1994). ATP is used in the cell as fuel for many metabolic reactions and functions. For example, ATP is used to maintain ion gradients in neurons. Under normal conditions, the intracellular K^+ concentration is 10 to 20

times higher than the extracellular concentration and Na^+ is maintained at a higher concentration outside of the neuron relative to inside. These ion gradients are created and maintained by an energy (ATP)-dependent Na^+-K^+ ion pump. A reduction in ATP levels causes dysfunction of the Na^+-K^+ ion pump which leads to a change in the ion repartition on either side of the membrane, hence a change of the membrane potential and depolarization. Depolarization of neuronal cells generates action potentials, which in turn trigger neurotransmitter release. When bound to their post-synaptic receptors, the released neurotransmitters cause further action potentials in postsynaptic cells and generate more neurotransmitter release (Hansen et al., 1982; Jiang et al., 1992; Silver and Erecinska, 1990). During ischemia, the supply of oxygen and glucose are limited, leading to a reduction of ATP synthesis by the mitochondria. Subsequently, elevated extracellular Glu levels due to ischemic effects on ATP induce further Glu release through activation of Glu postsynaptic receptors (Kimura et al., 1998), which mediate the influx of Ca^{++}, inducing depolarization and cell firing. Thus, high concentrations of Glu can cause neuronal cell death through a Glu-receptor-dependent pathway; this is referred to as excitotoxicity.

1.3.2 Excitotoxicity

1.3.2.1 Glutamate receptors

Glu receptors can be divided into ionotropic and metabotropic receptors. Ionotropic receptors are ligand (Glu)-gated cation ion channel receptors. The

binding of Glu and the co-ligand glycine to ionotropic receptors directly opens the channel, allowing the influx of ions such as Ca^{++} and Na^{+}, and a simultaneous efflux of K^{+}. Ionotropic receptors are divided into three subtypes defined by their affinity for different ligands: N-methyl-D-asparate (NMDA), α-amino-3-hydroxy-5-methyl-4-isoxasole (AMPA) and kainate. NMDA-binding receptors have relatively high Ca^{++} permeability, but under the normal resting neuronal membrane potential of -70 mV, the channel is blocked by Mg^{++}. When the neuron is depolarized, the Mg^{++} block is removed and NMDA receptors can be activated. Activation of AMPA and kainate receptors also causes the influx of Ca^{++} and Na^{+}. Metabotropic Glu receptors, on the other hand, are coupled to second messenger systems via G-proteins. The binding of Glu to metabotropic Glu receptors activates G-proteins, which in turn activate or modulate several intracellular signaling cascades. Reports in the literature have indicated that the metabotropic Glu receptors have little involvement in excitotoxicity.

1.3.2.2 Mechanism of excitotoxicity

NMDA receptor activation causes an ion imbalance, which can lead to osmotic change (hyperosmolarity) where water is drawn into the cell and ultimately causes the cell to burst, i.e. necrotic cell death. Activation of NMDA receptors can also induce apoptosis through increased cytosolic Ca^{++} concentrations activating Ca^{++}-sensitive proteases, protein kinases and phospholipids (Martin et al., 1998). Blockage of NMDA receptors with their antagonist MK-801 induces significant protection of brain cells under ischemic conditions *in vivo* (Buchan,

1990; Gill et al., 1988; Tremblay et al., 2000) and *in vitro* rescue of neuronal cells exposed to Glu toxicity (Tremblay et al., 2000). Cell death, induced in cultured cells by oxygen-glucose deprivation where cells were grown in medium without Ca^{++}, was blocked by treatment with an NMDA receptor antagonist, suggesting that Ca^{++} is not the only factor involved in NMDA receptor dependent cell death (Goldberg and Choi, 1993). A Na^{+} influx is probably also involved in this cell death process considering that administration of a Na^{+} channel blocker, QX-314, demonstrated significant neuroprotection in the *in vitro* model (Stys, 1998). Moreover, the Na^{+} channel blocker tetrodotoxin reduced the amount of cell death in cultured hippocampal cells which were oxygen-glucose deprived (Kimura et al., 1998).

The involvement of the non-NMDA receptors, namely AMPA and kainate receptors, in neuronal cell death induced by ischemia has also been suggested. The administration of the AMPA antagonist, NBQX, was reported to reduce significantly the number of hippocampal CA1 neurons lost in gerbils that underwent transient forebrain ischemia (Li and Buchan, 1993; Sheardown et al., 1993). Similarly, the administration of the kainate antagonist LY377770 to gerbils after induction of forebrain ischemia, and to rats after induction of focal ischemia, also significantly protected neurons in the CA1 region and reduced infarct size, respectively (O'Neill et al., 2000). These data show that NMDA, AMPA and/or kainate receptors play important roles in excitotoxicity induced by cerebral ischemia. Another major cell death pathway is also triggered by cerebral

ischemic damage and this pathway is independent of Glu receptors. This Glu-receptor independent cell death pathway is termed oxidative stress.

1.3.2.3 Oxidative stress

Oxidative stress is caused by accumulation of intracellular reactive oxygen species (ROS). Intracellular ROS can be increased by ischemia through several pathways, one of which is mediated by dysfunction of the cysteine-Glu antiporter, x_c^- (Sato et al., 1999). The antiporter x_c^- imports cysteine into cells in exchange for exportation of intracellular Glu. Imported cysteine is used to produce the free radical scavenger, glutathione (GSH). GSH is a three-amino acid peptide consisting of glycine, glutamate and cysteine and is the main molecule in neuronal cells to scavenge free radicals. High concentrations of extracellular Glu, induced by ischemic damage, inhibit x_c^- function and cause intracellular depletion of cysteine. Depletion of cysteine leads to the depletion of GSH and thus the accumulation of free radicals and ultimately cell death (Murphy et al., 1989).

Another important pathway to accumulate intracellular ROS concentration is to produce new ROS. In *in vivo* rodent models, during ischemic and the post-ischemic reperfusion periods, there is accumulation of ROS that exacerbates neuronal death. This increase of ROS was prevented by administration of monoamine oxidase inhibitors (MAOIs) (Suzuki et al., 1995; Tadano et al., 1995), suggesting that the ROS accumulation induced by ischemia or reperfusion is mainly, if not solely, due to MAO activity. In parallel, depletion of free radical scavengers was observed once blood flow was re-established (Vanella et al.,

1993), which coincided with accumulation of ROS. Therefore, the depletion of free radical scavengers observed during reperfusion is probably accelerated by ROS which are produced by MAO.

1.4 GABA in ischemia

γ-Aminobutyric acid (GABA) is the major inhibitory neurotransmitter in the vertebrate CNS. Once released, GABA binds to one of two GABA receptors, $GABA_A$ or $GABA_B$ receptors. $GABA_A$ receptors are ligand-gated Cl^- channel receptors and $GABA_B$ receptors are coupled to G-proteins. $GABA_A$ receptors possess several binding sites including a GABA binding site and a benzodiazepine binding site.

During ischemia, an accumulation of extracellular GABA has been observed *in vivo* (in hippocampus, striatum, and cerebral cortex of gerbil) and *in vitro* (rat hippocampal slices) (reviewed by Schwartz-Bloom and Sah, 2001). Schwartz-Bloom and Sah (2001) suggested that excitotoxicity induces the elevation of extracellular GABA through (i) the release of vesicular-containing GABA from GABAergic neurons during depolarization triggered by Ca^{++} influx, (ii) the secretion of GABA due to the reversal of the GABA transporter under depolarizing conditions, and (iii) the leakage of GABA from damaged GABAergic neurons.

Oxidative stress can also cause an increase of extracellular GABA. For example, published reports showed increased released GABA from hippocampal slices following H_2O_2 administration (Saransaari and Oja, 1998). Moreover,

increased concentrations of ROS, generated by administration of arachidonic acid, have been shown to decrease reuptake of GABA (Chan et al., 1983). These increases of GABA secretion induced by exitotoxicity and oxidative stress may indicate that damaged cells or neighboring cells are attempting to reduce the excitotoxic damage.

Indeed, reports in the literature show that increased brain GABA levels are neuroprotective. Treatment with either GABA agonists, GABA reuptake inhibitors or inhibitors of GABA catabolism (e.g. GABA-T inhibitors) have been shown to protect neurons in the CA1 hippocampal region from ischemic damage (Schwartz-Bloom and Sah, 2001) .

The increase of extracellular GABA induced by ischemia alone, however, is not sufficient to prevent neuronal cell death triggered by ischemic damage. The fact that physiological GABA accumulation in response to ischemia does not exert any significant protective effect may lie in either one or both of the following reasons. 1. The accumulation of GABA is transient compared to the accumulation of Glu and this difference in duration may contribute to a delayed cell death; or 2. increases in GABA levels are lower than the increase of Glu levels and thus is insufficient to rescue cells. Additionally, because ROS have been shown to decrease $GABA_A$ receptor density (Sah et al., 2002), it is possible that under ischemic conditions any beneficial effect of transiently elevated GABA levels is lost due to a lack of receptors.

1.5 Experimental models of cerebral ischemia

1.5.1 *In vivo* models

1.5.1.1 Transient forebrain ischemia

Several animal models have been developed in primates and rodents to study cerebral ischemia. The rodent models include various species such as mice, gerbils and rats. Mice are useful for generating genetically manipulated animals, although the larger sizes of rats and gerbils make them far more suitable models for surgical procedures (Johansen, 1993; Lipton, 1999). Gerbils are commonly used to model transient forebrain ischemia because these animals do not possess a complete Circle of Willis. Thus, in gerbils, two-vessel occlusion of the common carotid arteries is sufficient to induce a forebrain cerebral ischemia. In contrast, rats do possess a complete Circle of Willis and thus require four-vessel occlusion of the vertebral and common carotid arteries to produce similar ischemic damage. A two-vessel occlusion model is also used in rats to produce forebrain ischemic damage; however, the degree of damage is greatly reduced compared to that of the four-vessel occlusion model. Blood vessel occlusion can be achieved by ligation and/or cauterization. Because the ligation of a blood vessel can be reversed, ligation occlusion is best suited to produce transient ischemia and the study of reperfusion effects. The hippocampal CA1 region is the most vulnerable to transient forebrain ischemia.

1.5.1.2 Focal ischemia model

For models of focal ischemia, rats are typically the animal of choice. In this model, the middle cerebral artery (MCA) is permanently or transiently occluded. Occlusion is accomplished through a variety of means including insertion of a nylon thread into the MCA or placement of clot material at the junction of the MCA and internal carotid artery (Lipton, 1999). For the thread model, the duration of ischemia time can be manipulated by regulating the length of time the suture remains in place. For the permanent occlusion, the nylon thread is left in place for at least a day, while for transient occlusion, it is left for less than 3 hours. The removal of the thread after transient occlusion allows the study of the reperfusion effect.

Another method to model focal ischemia is the insertion of a pre-formed clot into the MCA. In this procedure, a small quantity of blood is withdrawn from the artery into a needle where a clot is allowed to form and the clot is then placed back into the artery by a catheter. Typically, the clot dissolves over a few hours time. This model mimics the human thromboembolic ischemia.

1.5.2 *In vitro* models

1.5.2.1 Brain slice models

To study ischemia *in vitro*, there are primarily two models used: brain slice models and cell culture models. Brain slices, particularly hippocampal slices, provide a useful model to study ischemic damage at the cellular level while

maintaining relatively intact cell-cell interactions. However, brain slice models are physiologically compromised compared to *in vivo* models since there is no blood supply and they are isolated from other tissue and organs.

1.5.2.2 Cell culture models

Cell culture models can use either primary or immortalized cell lines. Primary cell cultures are prepared from embryonic, neonatal or adult rodents, depending on the cell type desired, by dissociating the brain cells enzymatically and/or mechanically. The main advantages of primary cultures lie in their usefulness as a tool to conduct research at the cellular and molecular levels. Primary neuronal cultures, however, have limited life span (up to a few weeks) because of their non-dividing characteristics and are available in densities proportional to the amount of tissue which can be harvested. However, non-neuronal cells are always present to some degree in enriched neuronal cultures and will proliferate over time. Hence, the addition of mitogenesis inhibitors in cell culture medium is required to restrict the proliferation of non-neuronal cells. It is important to be aware that overdose or prolonged treatment of mitogenesis inhibitors can damage neurons.

Cell line cultures are prepared by hybridizing the target cells with cancer cells or viruses to immortalize the target cells. Immortalized cell lines present several advantages over primary cell cultures. First, they can proliferate so that they provide an unlimited number of the desired cells, a trait which is particularly valuable for neuronal cell lines. Second, their tolerance to cryopreservation

enables their storage and distribution among researchers, which allows several studies to be carried out on the same cell type in separate laboratories and at different time periods. Additionally, neuronal cell lines are free from non-neuronal cells; therefore, the analysis of pure neuronal cell behavior is possible. The main disadvantage of immortalized cells is that they present morphologic and biochemical characteristics different from their parent cells. For example, the HT-22 cells used in this thesis were derived from mouse hippocampal neurons that were immortalized by Henderson et al. (1989) with a temperature-sensitive retroviral vector (Frederiksen et al., 1988). HT-22 cells have been used to investigate the mechanisms of Glu toxicity; however, further studies revealed that the cells, unlike primary hippocampal neurons, do not express ionotropic or metabotropic Glu receptors (Davis and Maher, 1994). Subsequent studies showed that HT-22 cells were damaged from high concentrations of extracellular Glu through oxidative stress as a consequence of the depletion of GSH (Davis and Maher, 1994). To date, the GABAergic characteristics of this cell line have not been studied. Specifically, whether these cells possess GABA, the GABA synthesizing enzyme glutamic acid decarboxylase (GAD), the GABA catabolizing enzyme GABA-transaminase (GABA-T) and/or the two types of GABA receptors ($GABA_A$ and $GABA_B$ receptors) remains unknown. If they possess some or all of these characteristics, HT-22 cells could be used as a model system to examine the effects of GABAergic drugs on neurons under oxidative stress.

1.6 The use of MAOIs and GABAergic compounds in ischemia

Although lost functions caused by cerebral ischemia-induced neuronal cell death can be alleviated to some extent by rehabilitation, it is not surprising that large efforts have been put toward the development of neuroprotective drugs. As mentioned previously, in animal models of ischemia, NMDA, AMPA and kainate receptor antagonists were reported to possess neuroprotective properties (Gagliardi, 2000). Similarly, Ca^{++} or Na^{+} channel blockers have also been reported to exhibit neuroprotective properties in animal models (Buchan et al., 1994; Williams and Tortella, 2002; Cheung, 2003). In addition, estrogens and analogues, which act as antioxidant reagents, have also been shown to be neuroprotective in cell culture models of Glu excitotoxicity (Green et al., 2001; Gursoy et al., 2001; Prokai et al., 2001). A review of the wide variety of compounds which have been investigated for neuroprotective properties is beyond the scope of this thesis. Therefore, the following review focuses on MAOIs and GABAergic compounds.

1.6.1 MAOIs

In neuronal cells, MAO generates H_2O_2 from metabolism of catecholamines (for review, see Singer and Ramsay, 1995; Weyler et al., 1990). There are two forms of MAO, MAO-A and MAO-B, which share 70 % amino acid sequence identity. These enzymes have different substrate preference: MAO-A oxidizes the neurotransmitters serotonin and noradrenaline, while MAO-B preferentially reacts with benzylamine and phenylethylamine. Because MAO activity is responsible

for ROS production observed during the reperfusion period, it is anticipated that inhibition of MAO during or after ischemia would benefit neuronal cell survival.

Indeed, administration of selective and irreversible MAOIs to gerbils after induction of focal ischemia has been shown to prevent neuronal cell death (Ballabriga et al., 1997; Langston et al., 1984). In parallel, *in vitro* studies have demonstrated the neuroprotective properties of MAOIs in hippocampal neuronal cell line, HT-22 cells (Maher and Davis, 1996) and in cultured chick retina cells from glutamate cytotoxicity (Jacobsson and Fowler, 1999). Moreover, Todd et al. (1999) have shown that the MAOI phenelzine (PLZ) rescued hippocampal neurons from global ischemia-induced cell death in gerbils.

Recently, administration of the selective and irreversible MAO-B inhibitor rasagiline to rats was reported to significantly reduce the infarct region after focal ischemia (Speiser et al., 1999). Under Glu oxidative stress conditions, treatment of HT-22 cells with MAO-A inhibitors was reported to reduce the cell death, although the concentration of MAO-A inhibitors used in this study was so high that MAO-B activity was also inhibited (Maher and Davis, 1996).

1.6.2 GABAergic drugs

GABA hyperpolarizes post-synaptic neurons, hence the potential neuroprotective properties of GABA to neurons under ischemic conditions have been widely studied. In rodents, administration of sedative doses of diazepam, an agonist at the benzodiazepine binding site of the $GABA_A$ receptors, significantly increased neuronal cell survival in the hippocampus after an ischemic event, but at the

doses tested, a hypothermic effect was also observed (Johansen and Diemer, 1991; Schwartz et al., 1994). This was important as hypothermia itself has been shown to protect hippocampal neurons from global ischemia-induced damage in gerbils (Colbourne and Corbett, 1994). Maintaining the body temperature of ischemic animals at 36.5 °C resulted in a reduction, but did not eliminate, the neuroprotective effect of diazepam (Dowden et al., 1999). The $GABA_A$ receptor agonist muscimol was shown to induce hypothermia (Serrano et al., 1985) and to significantly reduce the infarct zone of ischemic rats (Lyden and Lonzo, 1994). In contrast, PNU-101017, a partial agonist at the benzodiazepine binding site, did not induce hypothermia, yet analyses showed it significantly protected neurons, even better than diazepam, in gerbils with transient forebrain ischemia (Hall et al., 1998).

In other studies, tiagabine, a GABA reuptake inhibitor, significantly reduced hippocampal cell death induced by transient forebrain ischemia (Inglefield et al., 1995). Tiagabine not only increased extracellular GABA levels, but also induced hypothermia. Further analyses showed that maintaining the animal's body temperature resulted in a significant attenuation of tiagabine's neuroprotective effects. These data suggest that the mechanisms through which tiagabine protects neurons from ischemia include hypothermia. In addition, other investigations showed that the GABA-reuptake inhibitor, CI-966, reduced ischemic damage and improved locomotor function compared to controls in the transient forebrain model of ischemia (Phillis, 1995).

Building on these experiments, our laboratory showed that a novel analogue and putative metabolite of PLZ, namely β-phenylethylidenehydrazine (PEH), which possesses GABA-T inhibitory effects, thereby increasing brain GABA levels (Parent et al., 2002), has neuroprotective effects on global ischemic damage (Todd et al., 1999).

As mentioned earlier, ischemia-induced high concentrations of extracellular Glu induces both excitotoxicity and oxidative stress. Although the effects of GABA on cells undergoing both excitotoxicity and oxidative stress have been widely studied, no study to date has shown the GABA effects on neuronal cells undergoing oxidative stress only.

1.7 PLZ, PEH and NAP

PLZ has been clinically used for the treatment of panic disorder, social phobia and depression (Kayser et al., 1988; Liebowitz et al., 1988) and is an irreversible and non-selective MAO inhibitor. Popov and Matthies (1960) and Baker et al. (1991) showed that PLZ also displays GABA-T inhibitory properties and, after systemic administration, can increase GABA levels in rat brain. The inhibitory effects of PLZ on GABA-T were reported to likely be due to a metabolite of PLZ produced by the actions of MAO (Popv and Matthies, 1969; Todd and Baker, 1995), and one potential metabolite suggested was PEH (Yu and Tipton, 1989) . Published reports showed that i.p. injection of PEH to rats and gerbils significantly inhibited GABA-T, but only weakly inhibited MAO (Paslawski et al., 2001; Todd et al., 1999). Our laboratory previously showed that both PLZ and

PEH have neuroprotective properties in the gerbil model of transient forebrain ischemia (Todd et al., 1999; Tanay et al., 2002). The mechanisms through which PLZ or PEH offer this neuroprotection is not yet understood. Therefore, it was of interest to investigate whether these drugs would protect neurons from oxidative damage induced by Glu or H_2O_2.

Another interesting compound tested was N^2-acetylphenelzine (NAP). NAP is a minor metabolite of PLZ and possesses MAO inhibitory effects as strong similar to that of PLZ but does not elevate brain GABA levels (McKenna et al., 1991). To date, the neuronal protective properties of this compound have not been studied. This work described in thesis is the first to investigate its effect on neuronal cells under oxidative stress.

1.8 Purpose of the project described in this thesis

The purpose of the research described in this thesis was to investigate whether PLZ and its structural analogues would protect or rescue HT-22 cells from Glu or H_2O_2 toxicity and the mechanism underlying the observed beneficial effects. The hippocampal neuronal cell line was chosen to eliminate glia and other non-neuronal cells as variables because they are vulnerable to Glu and H_2O_2 toxicity. Since PLZ and analogous drugs could exert their protective effects through a GABAergic mechanism, the first objective was to delineate the GABAergic characteristics of HT-22 cells. The presence of GABA in cells was measured by immunocytochemistry (ICC) and high performance liquid chromatography (HPLC). Western blotting and ICC were used to detect the presence of the

GABA synthesizing enzymes GAD_{65} and GAD_{67}. The neuroprotective properties of three structural analogues were investigated: PLZ (inhibits both MAO and GABA-T); PEH (inhibits GABA-T); and NAP (inhibits MAO). Two models of cytotoxicity, Glu and H_2O_2, were used to evaluate the drugs. Results showed that PLZ was the most potent drug against Glu toxicity and that the MAOI activity of PLZ is probably important for the neuroprotective effect.

It is hoped that the results from this research will lead to further biochemical and molecular studies to fully elucidate the mechanisms through which PLZ and its analogues protect neuronal cells from Glu-induced oxidative stress.

Chapter 2 Materials and Methods

2.1 Materials

2.1.1 Materials

HT-22 cells were kindly provided by Dr. D. Schubert (Salk Institute for Biological Studies, La Jolla, CA).

Table 2-1 Materials used for Western blotting and reagent preparation.

Item	Catalogue number	Company
Immuno-Blot PVDF membrane (0.2 μm)	162-0177	Bio Rad
Whatmann filter paper	05-714-4	Fisher Scientific
0.2 μm filter (bottle top)	SCGPT05RE	Millipore
0.8 μm filter (syringe top)	SLAA025LS	Millipore

2.1.2 Reagents

2.1.2.1 Chemicals

PEH and NAP were kindly provided by Drs. E. Knaus and R.T. Coutts (University of Alberta, AB).

Other chemicals were purchased from companies as indicated below. All the chemicals were of analytical grade except for those used in HPLC analyses, which of HPLC grade.

Table 2-2 Chemicals used for reagent preparation.

Chemical name	Catalogue No.	Company
ABC kit	K0355	DAKO
Acrylamide	15512-023	Invitrogen
2-amino ethylisothiouronium bromide (AET)	A-5879	Sigma-Aldrich
Antibiotic-Antimycotic	15240-062	Invtrogen
BCA kit consists of two reagents: Bicinchoninic Acid Solution Copper (II) Sulfate Solution 4% (w/v)	B-9643 C-2284	Sigma-Aldrich
Bis-acrylamide	161-0201	Bio-Rad
Bovine Serum Albumin (BSA)	A-8022	Sigma-Aldrich
Bromophenol Blue	B-0149	Sigma-Aldrich
Complete mini	1 836 153	Roche Diagnostics
DAB	BM516	Fisher Scientific
5,5'-Dithiobis-2-Nitrobenzoic Acid (DTNB/Ellman's reagent)	D-8130	Sigma-Aldrich
Dulbecco's Modified Eagles Medium (DMEM) with high glucose	12100-046	Invtrogen

EDTA	S311	EM science
ECL	RPN2106	Amersham Biosciences
Fetal Bovine Serum (FBS)	16000-044	Invitrogen
Fluoraldehyde	26025	Pierce Chemicals
Formalin Solution (10%)	SF100-4	Fisher Scientific
GABA	A-2129	Sigma-Aldrich
^{3}H-GABA		PerkinElmer Life and Analytical Sciences Inc.
Glucose-6-Phosphate (G-6-P)	G-7879	Sigma-Aldrich
G-6-P-Dehydrogenase (G-6-P-DH)	G-7878, G-8164	Sigma-Aldrich
Glutathione Reduced Form (GSH)	G-6529	Sigma-Aldrich
Glutamate (Glu)	G-8415	Sigma-Aldrich
Glutathione Reductase (GR)	105678	Roche Diagnostics
Glycerol	G33-500	Fisher Scientific
Hanks' Balanced Salt Solution (HBSS)	14170-112	Invitrogen
IGEPAL	I-3021	Sigma-Aldrich
K_2HPO_4	BP363-500	Fisher Scientific
KCl	P217B	Fisher Scientific
α-Ketoglutarate	K-3752	Sigma-Aldrich
KH_2PO_4	P284-500	Fisher Scientific

MEM Vitamin Solution	11120-052	Invtrogen
β-Mercaptoethanol	UN2966	BDH Lab
Na Deoxycholate	S-285	Fisher Scientific
Na_2HPO_4	S374-1	Fisher Scientific
NaCl	S640-3	Fisher Scientific
β-Nicotinamide Adenine Dinucleotide (NAD)	N-0505	Sigma-Aldrich
NAD-3'-Phosphate (NADP)	N-3886	Sigma-Aldrich
Normal Horse Serum (NHS)	26050-070	Invtrogen
Pancreatin	P-3292	Sigma-Aldrich
Phenelzine (PLZ)	P-6777	Sigma-Aldrich
Pyridoxal-5'-Phosphate (PLP)	P-9255	Sigma-Aldrich
Sodium dodecyl sulfate (SDS)	BP166-500	Fisher Scientific
Scintillation fluid	141349	Beckman Coulter
Tetrahydrafuran (THF)	T425-1	Fisher Scientific
Tri-n-Octylamine (TOA)	T-8631	Sigma-Aldrich
Triton X-100	LC26280-1	Labchem. Inc.
Trypan Blue (0.4%)	T-8154	Sigma-Aldrich
Tween 20	P-5927	Sigma-Aldrich

2.1.2.2 Preparation of Reagents

2.1.2.2.1 Cell culture medium

DMEM medium powder was dissolved in double distilled H_2O (ddH_2O), and the pH was adjusted to 7.3. To prepare complete medium, DMEM medium was supplemented with 10% (v/v) FBS, 1% (v/v) MEM vitamin solution and 1% (v/v) antibiotic-antimycotic. Complete medium was filter sterilized through a 0.2 μm buffer-top filter.

2.1.2.2.2 Preparation of drugs

Although PLZ is water-soluble, to use consistent vehicles for all drugs, PLZ, PEH and NAP were dissolved into dimethyl sulfoxide (DMSO) to a 1M concentration and aliquots of these stock solutions were kept at -20°C. At the time of use, the stock solutions were diluted in the cell culture medium to their final concentrations. The final concentration of DMSO in the culture medium did not exceed 0.01% (v/v) and at this concentration, DMSO did not affect cell viability. All control experiments contained 0.01% (w/v) DMSO. To prepare cell media that contained higher concentrations of PLZ, PLZ was directly dissolved into the complete medium to a concentration of 10 mM; however, to create consistent conditions, DMSO was added to a final concentration of 0.01% (w/v).

2.1.2.2.3 Pancreatin

Pancreatin, 25g, was dissolved in 4.5% (w/v) NaCl. Undissolved pancreatin was allowed to settle in overnight at 4°C. The next day the supernatant was filtered once to remove unsettled sediment and further filter sterilized through a 0.2 μm filtration system. Sterilized pancreatin was aliquoted into 2 ml volumes and kept at -20°C until use. At the time of use, 8 ml of HBSS was added to bring the total volume to a 10 ml working solution.

2.1.2.2.4 Stock solutions for GABA-T assay

10 mM NAD

100 mM GABA

50 mM α-ketoglutarate

10 mM AET

1M Tris buffer (pH 7.9)

2.1.2.3 Buffers

Phosphate buffered solution (PBS), pH 7.3: 8.1 mM Na_2HPO_4, 1.5 mM KH_2PO_4, 137 mM NaCl, 2.7 mM KCl.

TPBS: Tween 20 was added to PBS to final concentration of 0.1% (v/v).

RIPA buffer: 1% (w/v) IGEPAL, 0.5% (w/v) Na Deoxycholate, 0.1% (w/v) SDS prepared in PBS.

2 x Sample buffer: 0.5 M Tris-HCl (pH 6.8) 0.5 ml, Glycerol 0.4 ml, 10% (w/v) SDS 0.8 ml, β-Mercaptoethanol 0.2 ml, 0.05% (w/v) Bromophenol Blue 0.1 ml, ddH_2O to top up to 8 ml.

10 x Running buffer: (to be used, dilute to 1 x final concentrations) 10 g SDS, 30 g Tris, 144 g Glycine, ddH_2O to top up to 1 liter.

10 x Tris Buffered Saline (TBS) pH 7.5: (to be used, dilute to 1 x final concentrations) 250 mM Tris-HCl, 1.5 M NaCl.

5 x Transfer buffer: (to use, add methanol (MeOH) to 15% final concentration (v/v) and dilute to 1 x with ddH_2O) 15 g Tris, 72 g Glycine in ddH_2O to top up to 1 liter.

Phosphate buffer (PB): 143 mM Na_2HPO_4 (pH 7.4), 6.3 mM EDTA.

Triton X-HCl solution (THCl): 0.1% (v/v) Triton-X100 in 10 mM HCl.

PLP stock solution: 3.7 mg in 15 ml ddH_2O.

Homogenization buffer: 20% (v/v) glycerol, 0.13% (v/v) Triton-X100, 10% (v/v) GSH stock (30.7 mg in 10 ml ddH_2O), PLP stock solution (for final concentration in the buffer, see 2.2.5.1), 10 mM K_2HPO_4, and 143 mM EDTA, adjusted to pH 7.3 with 10% (v/v) glacial acetic acid.

Incubation buffer for GABA-T assay (prepared using the stock solutions, see 2.1.2.2.4): 1 µl ^{3}H-GABA, 37.5 µl of 1M Tris buffer (pH 7.9), 7.5 µl of 100 mM GABA, 15 µl of α-ketogluarate, 15 µl of NAD, 15 µl of AET and 60 µl ddH_2O.

TOA solution: 2.2 ml TOA, 22.8ml ethyl acetate, 49.2 ml ddH2O containing 850 µl phosphoric acid. Combine all chemicals and shake for 3-4 min. Centrifuge for 15 min to separate TAO (upper layer) from water phase (bottom layer).

SDS-polyacrylamide gel electrophoresis (SDS-PAGE) gel:

- 29:1 Acrylamide stock solution: 29:1 (w/w) Acrylamide:bis-Acrylamide was dissolved in ddH_2O and filtered through 0.45 µm filter to remove undissolved powder and degassed under vacuum.

- 10% (w/v) Ammonium Persulphate (APS): 10% APS solution was prepared in ddH_2O and stored at -20°C until use.

- SDS-PAGE separation gels:

Separation gel conc.	10% (ml)	15% (ml)
ddH_2O	3.8	2.2
29:1 Acrylamide solution	3.3	5
1.5 M Tris-HCl (pH 8.8)	2.6	2.6
10% (w/v) SDS	0.106	0.106
10% APS	0.04	0.04
TEMED	0.02	0.02

2.1.3 Antibodies

Table 2-3 Antibodies used in Western blotting and immunocytochemistry.

Antibodies	Catalogue No.	Company
Microtubule associated protein 2 (MAP2)	M-4403	Sigma-Aldrich
GABA	AB141	Chemicon
Actin	CP01	Oncogene
Rabbit anti glutamic acid decarboxylase $(GAD)_{65/67}$ antibody	AB1511	Chemicon
Bcl-xl	2762	Cell Signalling
Biotinylated anti mouse IgG antibody	E0354	DAKO
Anti rabbit IgG HRP conjugated antibody	NA934V	Amersham
Anti mouse IgG HRP conjugated antibody	NA931V	Amersham

2.2 Methods

2.2.1 Cell culture

HT-22 cells were cultured in 10 ml of complete medium in a 75 cm^2 flask. The medium was replaced every 2 days. Cells in 75 cm^2 flasks were maintained under 50% confluence and were harvested with 10 ml working solution of

pancreatin. After 5 min incubation at 37°C with pancreatin solution, the cell suspension was transferred to a 15 ml conical tube and pelleted by centrifugation at 2,000 rpm (600 x g) for 5 min. The cell pellet was resuspended into complete medium and plated on appropriate plates.

2.2.2 Immunohistochemistry

All procedures were performed at room temperature (RT) unless otherwise stated. Cells grown on 6-well plates were rinsed with PBS for 3 min and fixed with 10% formalin for 10 min. Cells were then rinsed with ddH_2O for 3 min. Cell membranes were permeabilized with TPBS for 30 min. Following a rinse with PBS for 3 min, the cells were blocked with 10% (v/v) NHS in TPBS for 30 min. The primary antibody dilutions used were as follows: anti-MAP2 antibody 1:350 (v/v); anti-GABA antibody 1:1000 (v/v); anti $GAD_{65/67}$ 1:1000 (v/v). Antibody solutions were prepared with TPBS supplemented with 10% (v/v) NHS and incubated with the cells overnight at 4°C. The cells were then rinsed with PBS for 3 min and incubated with the secondary antibody (biotinylated anti mouse IgG; 1:200, v/v) for 30 min. After a 3 min rinse, the presence of the antigen was labeled with the Avidin-Biotin complex (ABC kit, Dako, used according to the manufacture's instructions) for 30 min. The ABC kit consists of avidin and biotin; they form a complex and are conjugated with horseradish peroxidase (HRP). This complex binds to the biotin of the secondary antibodies to enhance the primary immunoreaction. The immunoreaction was visualized using DAB with 0.3% H_2O_2. DAB was dissolved in ddH_2O according to the manufacturer's

instructions and filtered through a 0.8 μm filter to remove undissolved DAB. Added H_2O_2 is converted by HRP to oxygen and water, and oxygen converts soluble DAB to an insoluble form indicating the existence of antigen protein. Excess DAB solution was washed with PBS. Negative controls were obtained by omitting the primary antibody in the first incubation.

2.2.3 Western blotting

2.2.3.1 Sample preparation

Total protein extracts were prepared by lysing the cells with RIPA buffer. Specifically, cells were grown on 12-well plates to a density of $5x10^4$ cells/well for one day and harvested by incubation and scraping with 500 μl/well RIPA buffer. Protein assays were performed on cell extracts with a BCA kit (Sigma-Aldrich) according to the manufacturer's instructions. Cell lysates were diluted 10 times in ddH_2O to lower the SDS concentration of the RIPA buffer; SDS reacts with the components of the BCA kit and gives high background which makes the determination of protein difficult. Standard curves were generated from the dilution of a 10 mg/ml BSA stock in PBS. The BSA stock was diluted with 10% RIPA buffer in ddH_2O to 0.1, 0.2, 0.5, and 1 mg/ml final concentrations. To 10 μl of either samples or standards, 200 μl of BCA kit mixture were added. Samples/standards mixed with BCA reagents were incubated at 37°C for 30 min and the absorbance was measured at 562 nm. To prepare the protein samples for Western blotting, the cell lysates were diluted with 2 x sample buffer to a final

concentration of 2 µg/µl total protein and boiled for 10 min prior to loading onto SDS-PAGE gels.

2.2.3.2 SDS-poly acrylamide gel electrophoresis (SDS-PAGE) and Western blotting

To investigate the presence of $GAD_{65/67}$, $GABA_A$ or $GABA_B$ receptors, cleaved caspase-3, and Bcl-xL in HT-22 cells, a 75 cm^2 flask culture containing semi-confluent HT-22 cells was scraped and the cells were collected. To measure the amount of Bcl-xl, HT-22 cells were plated on a 24-well plate at density of $5x10^4$ cells/well. The next day the cells were preincubated with either vehicle or PLZ for one hour followed by Glu treatment with/without PLZ for 1, 2, 4, 8 and 16 hours. Cells were lysed in ice-cold RIPA buffer supplemented with protease inhibitors (complete mini, Roche) before assaying the cell lysate for protein content and boiling an aliquot with 2 x sample buffer.

The presence of $GAD_{65/67}$ was screened via a 10% SDS-PAGE gel whereas Bcl-xL and cleaved caspase 3 was screened through a 15% SDS-PAGE gel to have better separation of proteins around the targeted size (65 and 67 kDa for $GAD_{65/67}$, and 35 kDa for Bcl-xL). 30 µg of total protein extract was loaded per lane to investigate the expression of $GAD_{65/67}$, 10 µg for Bcl-xl and 100 µg for cleaved caspase-3. The electrophoresis was conducted in 1 x running buffer at 60 V first to allow the compression of the protein samples at the edge of stacking gel, then at 100 V for separation. After separation, the proteins were transferred onto PVDF membranes. PVDF membranes were wetted with 100% MeOH and

soaked in transfer buffer prior to their use in the transfer procedure. The transfer was carried out either in 1 x transfer buffer at 100 V for one hour at 4°C, or at 30 V overnight at RT. Once the transfer was completed, the membranes were blocked in TBS with 0.1% Tween 20 (TTBS) containing 5% (w/v) skim milk powder (TTBS-milk) for 30 min at RT with gentle agitation; they were then incubated with the appropriate primary antibody diluted in TTBS-milk overnight at 4°C. The next day the membranes were washed for 10 min with TTBS 3 times and incubated with HRP conjugated secondary (I:2000, v/v) antibody in TTBS-milk for 30 min at RT. Following the three 10 min washes with TTBS, the antigen was detected by ECL kit (Amersham) according to the manufacturer's protocol. ECL is a chemi-luminescent substrate. The reaction with ECL and HRP on secondary antibody results in emission of chemi-luminescence, which can be visualized by exposure to X-ray film.

The Western blotting bands visualized on X-ray film were then scanned and protein amount was measured by density of its immunoreactivity using MCID Elite 7.0 program (Imaging Research Inc. Ontario, Canada). The protein amount was then corrected using actin immunoreacted band as a standard protein for loading.

2.2.4 Cell viability test

HT-22 cells were harvested using pancreatin and plated onto 96-well plates at $2.5x10^3$ cells per well with 100 µl complete medium. The following day, the cells were preincubated with several concentrations of either PLZ (concentration

range 0.01-320 μM), PEH (concentration range 0.01-100 μM) or NAP (concentration range 0.01-320 μM) for one hour. The medium was then replaced with fresh medium containing the same concentration of drug and either Glu (5 or 10 mM) or H_2O_2 (20 μM) and incubated at 37°C for 24 hours. Cell viability was assessed by 3-(4,5-dimethyldiazol-2-yl)-2,5-diphenyltetrazolium bromide (MTT) at the end of the 24 hour incubation. MTT is a water-soluble tetrazolium salt which is metabolized in the mitochondria to an insoluble formazan salt dye. 10 μl of 5 mg/ml MTT solution was added to the medium after 20 hour of incubation and the cell culture was incubated for a further 4 hours. At the end of the 24 hour incubation period, the media was removed by aspiration and 100 μl DMSO was added to the wells to dissolve the insoluble dye. The optical absorbance due to the presence of the dye was measured at 570 nm. One experimental group consisted of 6 wells per experiment and the experiments were repeated at least 4 times. The results of the cell viability assay obtained by the MTT method showed a good correlation with the results obtained from the trypan blue assays. The trypan blue assay was carried out by replacing the medium of each well by 0.4% trypan blue solution and staining the cells for 10 min. The cell membranes of dead/dying cells are compromised such that trypan blue dye can penetrate through the membrane and stain the cytosol whereas alive/healthy cells are not stained by the dye. Hence, trypan blue staining is widely used to visualize and distinguish dead/dying cells. The trypan blue staining method is quite time consuming since positive and negative cells have to be counted and therefore this assay is not practical when evaluating a large volume of cells and plates.

Therefore, the MTT assay was chosen to assess cell viability for the studies in this thesis. To investigate a possible transient neuroprotective effect of the drugs, the medium was replaced with fresh complete medium without either toxin or drug following the initial 24 hour incubation with toxin and drug and the cells were further incubated 24 hours. At end of the second 24 hour incubation period, cell viability was measured with MTT assay.

2.2.5 Glutathione assay

The glutathione (GSH) assay method described by Teitze (1969) and as modified by Neumann et al. (2003) was used to determine the concentration of GSH in cultured cells grown in 96-well plates. The original method (Teitze, 1969) determined GSH concentration using an enzymatic reaction (Fig. 2-1). GSH is the reduced form of glutathione; it reacts with DTNB to generate 5-thiobis-2-nitrobenzoate (TNB). In detail, GSH reduces the binding of DTNB to yield a TNB and glutathione-bound TNB. The glutathione-bound TNB then again reacts with GSH, resulting in another TNB and oxidized glutathione (GSSG). GSSG is reduced again by glutathione reductase (GR) with concomitant oxidation of NADPH to $NADP^+$. TNB has a yellow color at neutral pH, and its absorbance peaks at 405 nm. The rate of increase of absorbance at 405 nm as a result of the reduction of DTNB is proportional to the concentration of GSH/GSSG in the cell. The relationship between the concentration and the rate of change of absorbance is rectangular-hyperbolic, and an unknown concentration can thus be determined by applying a Michaelis-Menten equation.

To perform the assay, cells were lysed in 10 mM HCl solution containing 0.1% Triton-X100 (THCl). The importance of using an of acidic solution is emphasized in several articles (Roberts and Francetic, 1993; Thioudellet et al., 1995); an acidic solution inhibits γ-glutamyltranspeptidase (GGT), an enzyme responsible for catabolism of GSH. Roberts and Francetic (1993) also reported that sample storage at -70°C for a year did not affect the quantification of GSH amount measurement by its activity. For the work described here, the assay was carried within one week of sample collection, and no significant change in GSH amount was noted during upon storage (data not shown).

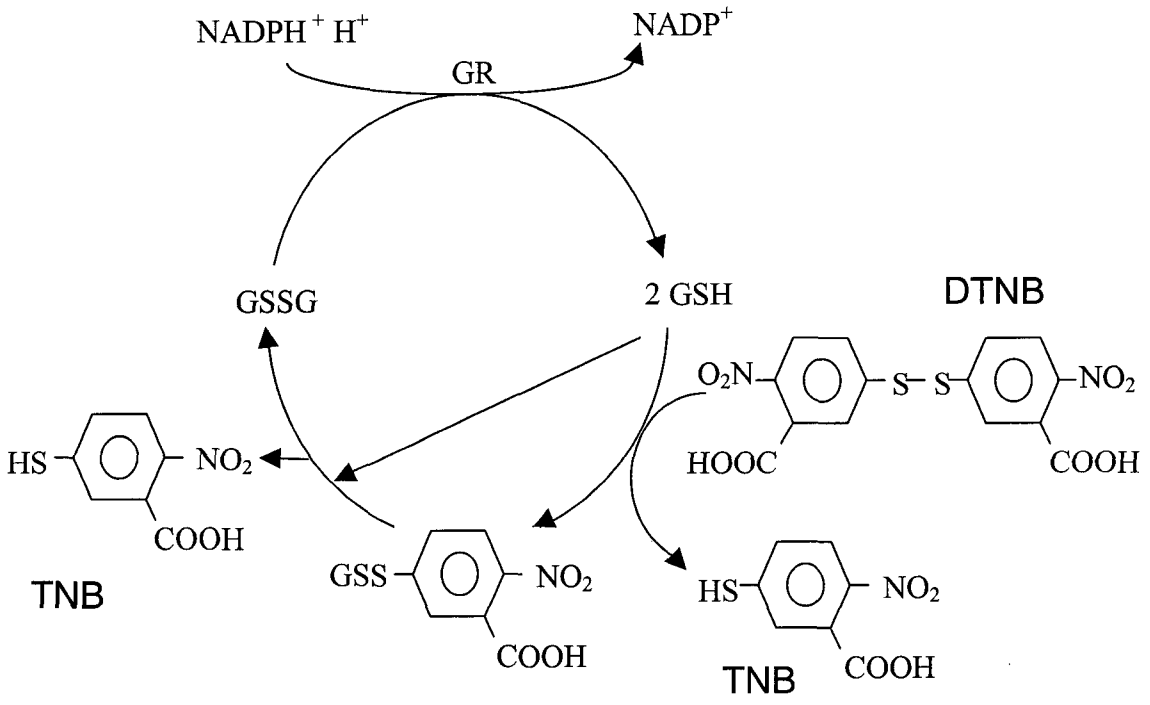

Figure 2-1 Scheme of glutathione recycling system.
Adapted from Neumann et al. (2003)

2.2.5.1 Establishing GSH assay conditions

Paradoxically, a high concentration of NADPH in the GSH assay is desirable to obtain the large amount of end product (TNB), yet a high concentration of NADPH can inhibit the enzymatic reaction. To counter this problem, Neumann et al. (2003) introduced an NADPH regeneration system to the reaction (Fig. 2-2). However, upon following the procedure and measuring the change in absorbance at 405 nm over time, which reflects the production of TNB, no positive results were detected.

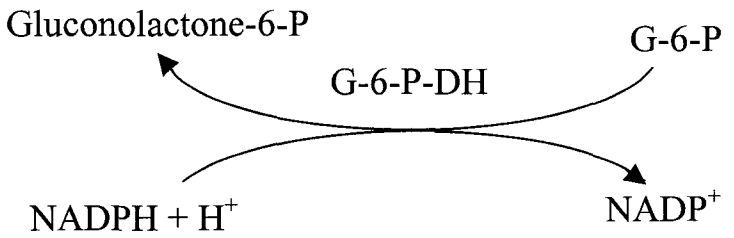

Figure 2-2 Schematic representation of the NADPH-regenerating reaction system. Glucose-6-phosphate (G-6-P) is converted to gluconolactone-6-phosphate by glucose-6-phosphate-dehydrogenase (G-6-P-DH) concomitantly with the conversion of NADPH to $NADP^+$. Adapted from Neumann et al. (2003).

Several experiments were then undertaken to determine the source of the problem. In order to determine whether GSH could react directly with DTNB, GSH was dissolved in 10% THCl in PB to several concentrations sampling from 0 to 75 µM and mixed with 4.9 mM (final concentration) DNTB. The solution turned bright yellow, with the absorbance at 405 nm proportional to the concentration of GSH. Next, to examine whether NADPH was being produced

by the $NADP^+$ cycling, 0.17 mM $NADP^+$ was added to 1.7 mM G-6-P and 5 U/ml G-6-P-DH in PB. Immediately after mixing, absorbance at 340 nm (indicating the production of NADPH) was measured; again no change of absorbance over time was observed. Since the concentration of G-6-P-DH may have been so high that the reaction could have run to completion before measurement began, a 10-fold lower concentration of G-6-P-DH was used to slow down the reaction. However, no change of absorbance at 340 nm was observed over time. Therefore I concluded that G-6-P-DH had lost its enzymatic activity. Given the negative results obtained, the $NADP^+$ cycling step was eliminated.

A GSH cycling step tested with a final standard concentration of GSH between 0 and 64 µM yielded acceptable enzymatic activity. In the presence of 40 µl of 5 U/ml GR in PB, 40 µl of 4.9 mM DTNB in PB, and 50 µM NADPH in PB were added to each well. The absorbance at 405 nm was measured every 10 sec after a brief mixing. The results (Fig. 2-3) showed a rapid increase in absorbance at lower concentrations of GSH while the reaction at higher concentration of GSH seemed to be completed even before any measurement was made. Reducing the GR concentration by 10-fold slowed the rate of product formation and was adequate for the preparation of standard curves (Fig. 2-3). Under the initial conditions, the mixing of 100 µl of THCl solution and 4.9 mM DTNB in PB resulted in a white cloudy solution. This cloudiness disappeared with the addition of GR and NADPH solutions, but enzyme activity and a change of absorbance were not observed in any control wells. From these observations,

40 µl of THCl were used for preparing the cell lysates and GSH standards, and a concentration 0.5 U/ml of GR was chosen for the subsequent assays.

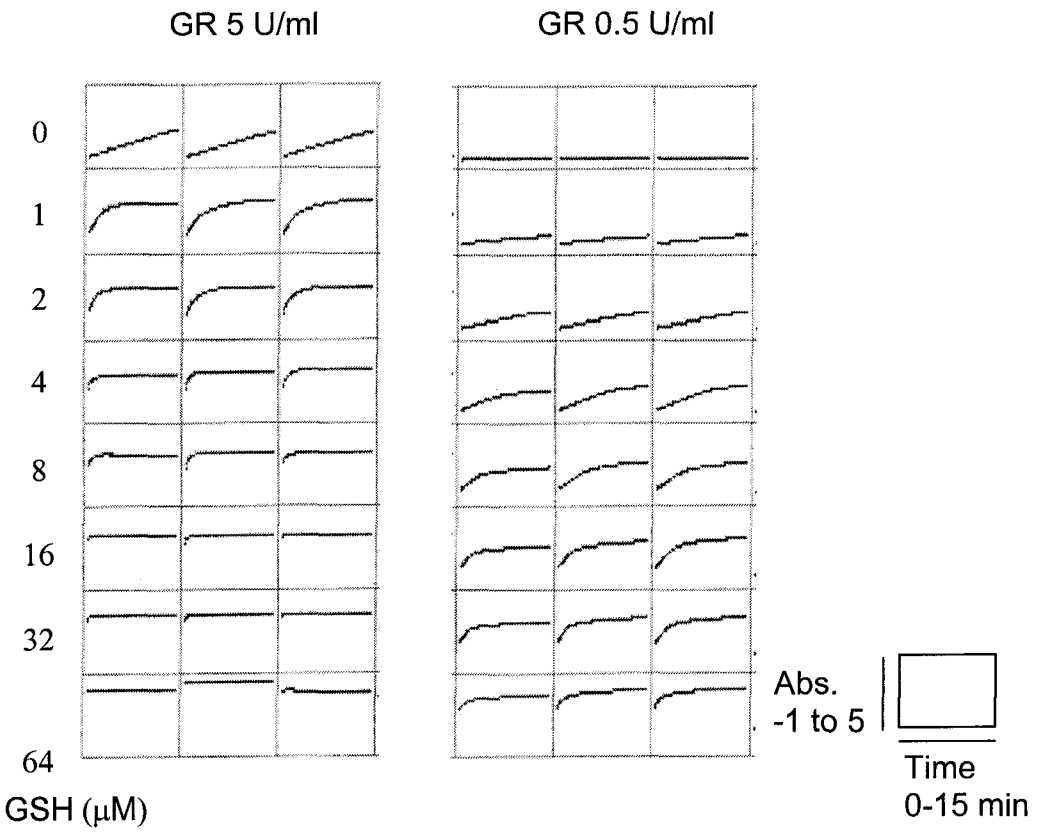

Figure 2-3 Comparison of the effects of GR concentration and GSH concentration on absorbance of GSH standards over time.

The absorbance was measured every 10 seconds over a 15 min period.

The final procedure used to determine GSH was as follows: HT-22 cells were plated on 24-well plates at a density of $5x10^4$ cells/well. The next day the cells were preincubated with either vehicle or 100 µM PLZ for one hour followed by incubation with either 5 or 10 mM Glu in the presence or absence of PLZ for 1, 2, 4, 8 and 16 hours. The cells could not be collected at the 24-hour incubation

time because most of the cells in Glu treatment group were dead and therefore the assay of GSH concentration was impossible. The cells were harvested by scraping the culture well with 500 µl ice-cold THCl. 20 µl (plus 20 µl THCl to make total volume as 40 µl) or 40 µl of cell lysate were aliquoted in triplicate in a 96-well plate, added with 40 µl of 4.9 mM DTNB/PB and 40 µl of 0.5 U/ml GR/PB. The reaction was started by the addition of 50 µl of 50 µM NADPH and, following brief shaking, the absorbance at 405 nm was measured every 10 seconds over a 15 min period. To draw the standard curves, mean rate of kinetic for the standards were obtained and plotted and an equation data point fit was generated to estimate GSH concentration (Fig. 2-4). The concentration of GSH in the samples calculated from the equation was corrected for the protein content of the cell lysate. 10 µl of cell lysate were assayed for protein content by mixing with 200 µl BCA kit solution and the absorbance at 562 nm was measured after 30 min incubation at 37°C. The presence of THCl did not interfere with BCA protein assay kit (data not shown).

The GSH measurements for each time point were repeated at least 5 times.

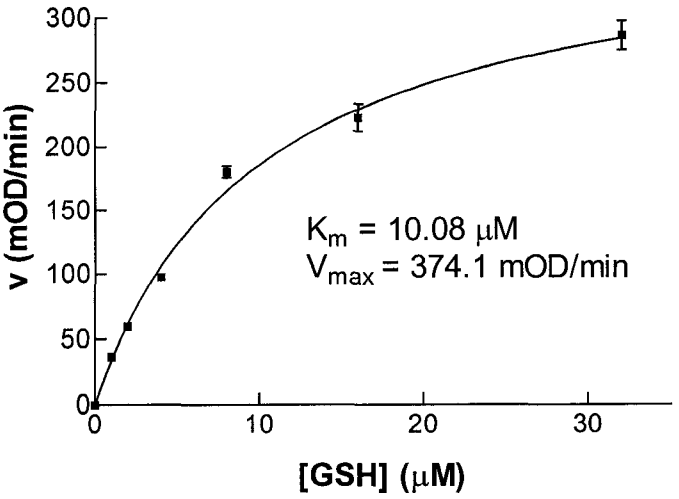

$$v = (374.1 \times [GSH]) / (10.08 + [GSH])$$

$$[GSH] = (10.08 \times \{v - blank\}) / (374.1 - \{v - blank\})$$

Figure 2-4 Michaelis-Menten plot of GSH turnover by GR.

Figure is shown as an example of plotted standard curve and deducted equation to calculate the GSH concentration in the samples.

2.2.6 HPLC assay

HT-22 cells were rinsed with PBS and scraped from 75 cm^2 culture flasks. The excess PBS was removed after centrifugation. Cell pellets were immediately frozen and kept at -80°C. At the time of the assay, the cell pellets were resuspended in 50 µl PBS and 20 µl of cell suspension were homogenized with 40 µl methanol. After a 10 min incubation on ice, the cell lysate was centrifuged at 9,168 x g at 4°C for 4 min to precipitate the proteins. GABA was analyzed using a reversed-phase HPLC/fluorescence detector system, as described by Parent et al. (2001). Briefly, the HPLC system consisted of a Waters Alliance

2695 XE pump and sample management system connected to a Waters 474 Scanning Fluorescence detector. The data were analyzed with Millennium version 2000 software (Waters, Milford, MA, USA). A 5 µl sample, standard or blank solution that were kept at 4°C were taken up and 5 µl of fluoroaldehyde reagent were added. Fluoroaldehyde reagent contains 2-mercaptoethanol and *o*-phthaldialdehyde (OPA). OPA reacts with the amino acids and GABA, and using 2-mercaptoethanol as a reducing reagent forms a highly fluorescent thioalkyl substituted isoindole that can be detected by the fluorescence detector. Chromatographic separations were performed on a Waters Spherisorb ODS 2, C-18 reversed-phase column (250×4.6 mm, 5 µm particle size) connected to a Waters uBondapak C_{18} pre-column. The column was kept at 30°C with a flow rate of 0.5 ml/min. The mobile phases were as follows: mobile phase A; 240 ml methanol, 0.08 M NaH_2PO_4, 20 ml acetonitrile, and 10 ml THF in 900 ml ddH_2O adjusted to pH 6.2 with NaOH, and mobile phase B; 1100 ml methanol, 0.04 M NaH_2PO_4, 60 ml THF in 1340 ml ddH_2O adjusted to pH 6.2 with NaOH. Both mobile phases were filtered with 0.25 µm filter and degassed under vacuum. The ratio of mobile phase was 40% A and 60% B initially and a gradient was run over the next 40 min, with a final mobile phase concentration of 100 % B. After 40 min, the gradient was returned to the initial condition and the gradient was maintained for at least 20 min to condition the column for the next run. The fluorescence detector had the excitation and emission wavelengths set at 260 and 455 nm, respectively. To determine the retention times of GABA, a standard

solution of GABA was prepared in methanol: H_2O_2 solution (1:2) and run on the system in the described condition. Retention time of GABA was approx. 20 min.

2.2.7 GABA-T assay and troubleshooting

The GABA-T assay reported by Paslawski et al. (2001) was slightly modified for HT-22 cells. GABA-T activity was measured by the analyzing the metabolite formed from GABA. In tissue, GABA-T converts GABA and oxoglutarate to succinic semialdehyde and Glu; succinic semialdehyde is converted to succinate by endogenous succinic semialdehyde dehydrogenase in the presence of NAD. GABA was radiolabelled with tritium (^3H); thus the generated succinate is also ^3H labeled. ^3H-succinate is then extracted into a liquid anion exchanger (tri-n-octylamine, TOA). In normal cellular metabolic conditions, Glu formed from GABA by GABA-T at the first step can be used to generate new GABA. For this GABA-T assay, formation of new ^3H Glu from ^3H GABA was prevented by addition of a sulphydryl reagent, dithiothreitol.

HT-22 cells were rinsed with PBS and scraped from 75 cm^2 flask. Collected cells were pelleted and stored at -80°C until assay. For the assay, the cells were homogenized in 50 µl homogenization buffer. 10 µl of cell lysate was mixed with 20 µl incubation buffer and incubated in a 37°C water bath for 30 min. After the incubation, the samples were placed on ice, 100 µl TOA was added and the samples were successively vortexed for 5 sec, then centrifuged for 5 min at 11,000 rpm at 4°C. The supernatant was placed in scintillation vial containing 4 ml scintillation fluid and the decay of radioisotope was counted.

HT-22 cells from a semi-confluent 75 cm^2 flask did not show any GABA-T activity (data not shown); the protein amount may have been too low for detection. The assay protocol used here was developed to measure the GABA-T activity in rat brain homogenates (Baker et al., 1991). The results from the protein assay showed that the protein concentration of the cell lysate was about 1/10 of that of brain homogenate. To examine my procedural skill, I measured GABA-T activity in gerbil brain. Gerbil brain was homogenized in 20 volumes (w/v) homogenization buffer and the procedure described earlier was followed. Fig. 2-5 shows that GABA-T activity was successfully detected and its activity could be inhibited by the addition of 10 μM PLZ to the homogenates as reported previously (McKenna et al., 1991). Therefore, the negative results were not due to technical error. Increasing the protein amount by increasing the number of cells (hence the number of flasks) would make the experimental plan rather time consuming and costly. Reducing homogenization buffer was also not feasible because the homogenization in less volume of buffer than 50 μl was technically difficult. Thus, I attempted to increase the activity of GABA-T by increasing PLP. PLP is a co-enzyme for GABA-T. An increase of PLP might increase the efficiency of GABA-T activity from the original 1 mM to higher, such as 5 or 10 mM, hence an increase in the amount of final product. However, results showed that the higher the concentration of the PLP, the lower the amount of radioactivity detected (Fig. 2-5). After many successive attempts to determine GABA-T activity in HT-22 cell lysates failed, determination of whether mRNA for the protein was present in the cells was undertaken.

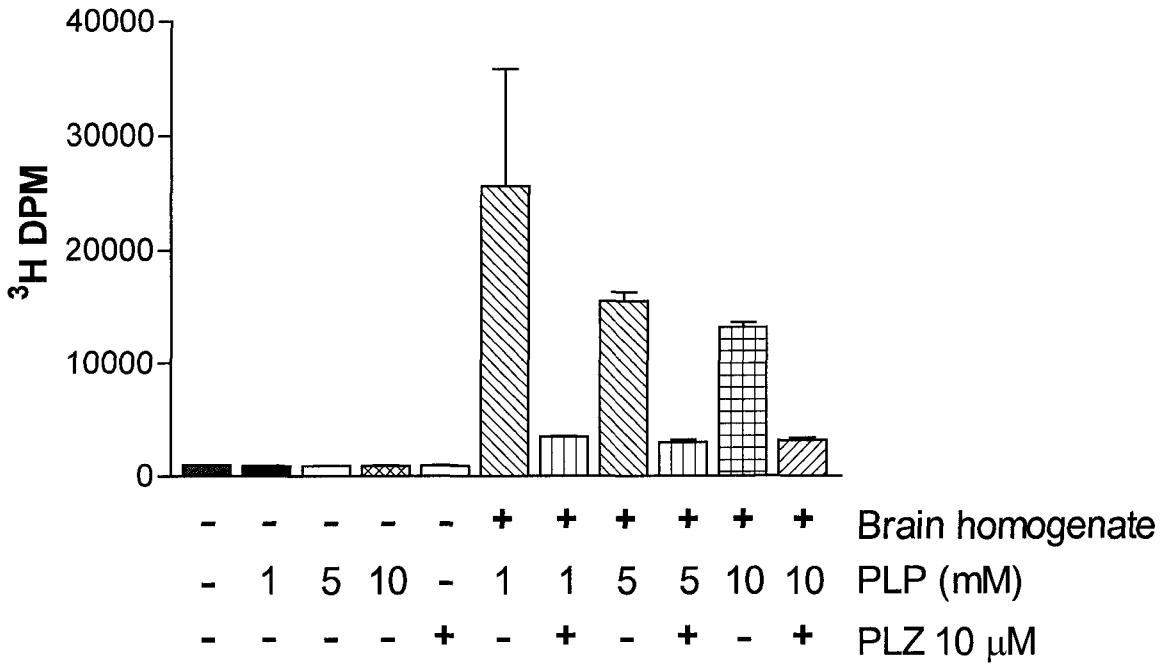

Figure 2-5 GABA-T activity measurement in gerbil brain.

GABA-T activity in gerbil brain was detected and the activity was suppressed by addition of 10 μM PLZ. The administration of higher concentration of PLP lowered the GABA-T activity. ^{3}H decay per minute (DPM) represents the amount of ^{3}H succinate.

2.2.8 GABA-T RT-PCR

Since the presence of GABA transaminase within HT-22 cells could have been missed by the techniques previously used, we sought to investigate whether HT-22 cells expressed GABA-T by searching for the presence of its mRNA by reverse transcription (RT)-PCR. The cDNA sequence of rat GABA-T previously published (Medina-Kauwe et al., 1994) was used as a reference sequence to query the mouse cDNA database for the orthologous sequence using NCBI

BLAST. The mouse cDNA sequence found {gi|35192986|gb|BC058521.1 (Strausberg et al., 2002)} was homologous to that of the rat (>95% sequence identity) and was used to design PCR primers. The 5' primer corresponded to the sequence 215-244, (5'-CAGCCAAGCCGCTGCCAAAGTTGACATTGA-3') and the 3' primer was designed from the sequence 1060-1088 (5'-AGGAAGCTGAGAGACATAGCCAGGAAGCAT -3') as 5'-ATGCTTCCTGGCTATGTCTCTCAGCTTCCT-3'. HT-22 cells were grown to confluence in a 100mm Petri dish, and total RNA was isolated. In order to minimize the number of optimization steps required to obtain an eventual positive result, the reverse transcriptase step was performed using InVitrogen Superscript II™ Reverse transcriptase according to the manufacturer's instructions, while the PCR step involved the side-by-side comparison of the amplification efficiency of several PCR kits manufactured by different companies such as Invitrogen (Taq Polymerase), Stratagene (ProStar UltraHF RT-PCR system), Promega (Taq DNA Polymerase in storage buffer B) and Eppendorf (HotMaster™ Taq Polymerase). Each kit was used according to the respective manufacturer's instructions. The magnesium concentration was adjusted to 1.5 or 3mM for the reactions set with either InVitrogen or Promega kits and a total of 12 reactions were set up for each kit-condition combination. The 1250 μl PCR reactions were aliquoted in a 96-well plate and the amplification was carried out by an Eppendorf Mastercycler® Gradient thermal cycler programmed for the following amplification conditions: initial denaturation 94°C 2min; cycling denaturation 94°C 1min; annealing

55±10°C 1min; elongation 68°C 1min; 40 cycles; final elongation 68°C 5min; cooling to 4°C.

RT-PCR was kindly performed by Dr. Véronique Tanay.

2.3 Statistical analysis

The data obtained in this thesis were analyzed using one-way Analysis of Variance (ANOVA). Where main effects were identified, Tukey's post test was used to detect group differences. A significance value of $P<0.05$ was chosen to identify statistical significance.

Chapter 3 Results

3.1 HT-22 cells exhibit neuronal character

Microtubule associated protein 2 (MAP2) is a widely used neuronal protein marker that has been shown to localize at the dendrites and perykarya of neuronal cells but not in non-neuronal cells (De Camilli et al., 1984). In order to demonstrate the neuronal characteristics of HT-22 cells, cells were immunostained for the presence of MAP2 (Fig. 3-1).

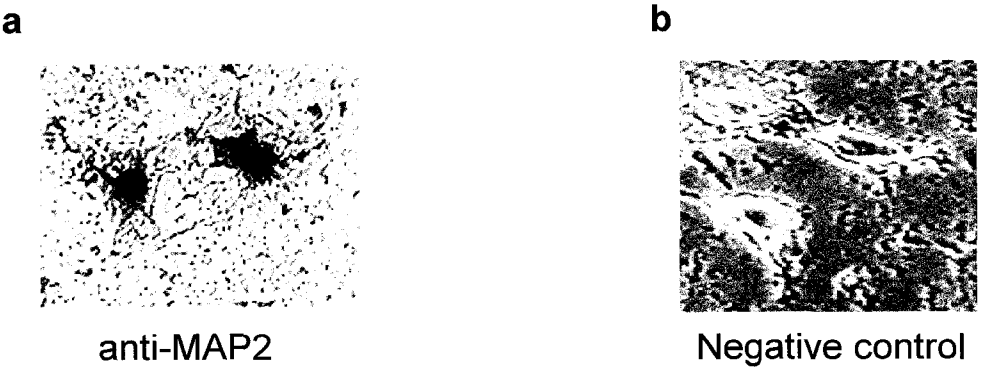

Figure 3-1 Immunocytochemical analysis of MAP-2 in HT-22 cells

HT-22 cells were immunoreacted with antibodies recognizing MAP-2 protein and visualized with DAB. Plate a shows positive MAP2 immunostaining. Plate b shows the negative control.

3.2 HT-22 cells express GABA and $GAD_{65/67}$ but not GABA-T

The GABAergic properties of HT-22 cells were also examined by immunocytochemistry using anti-GABA and anti-$GAD_{65/67}$ antibodies. HT-22 cells were positive for both GABA and $GAD_{65/67}$ (Fig. 3-2). To further confirm that HT-

22 cells contain GABA, HPLC analyses of both cell lysates and cell media were performed. Results from cell lysates showed that after extraction, a peak of retention time coinciding with that of a standard GABA solution was observed (Figs. 3-3). GABA was also detected by HPLC in the cell culture medium; therefore HT-22 cells likely possess a mechanism to secrete GABA.

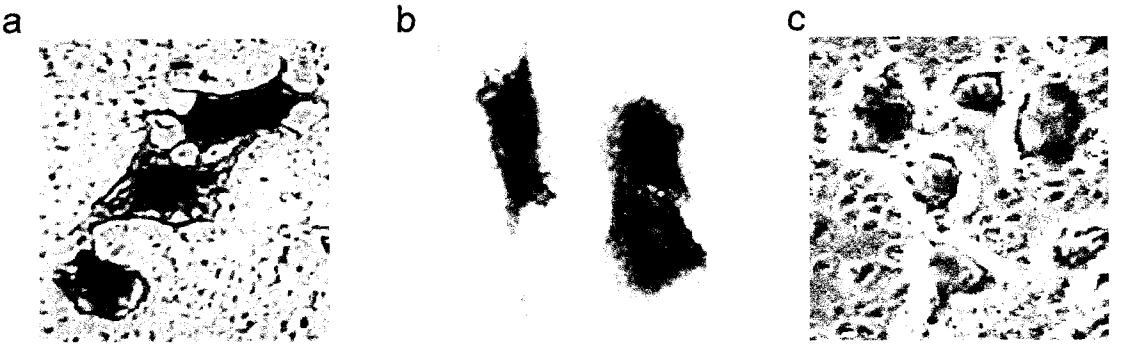

Figure 3-2 Immunocytochemical analysis of GABA and $GAD_{65/67}$ in HT-22 cells.
HT-22 cells were immunoreacted with antibodies recognizing GABA (Plate a) or $GAD_{65/67}$ (Plate b) and visualized with DAB. Negative controls were the primaty antibodies were omitted were run with each assay (Plate C). HT-22 cells were positive for both GABA and $GAD_{65/67}$.

Confirmation of the presence of $GAD_{65/67}$ proteins was performed using Western blotting of HT-22 cell homogenates and including fresh homogenate from mouse hippocampus as a positive control. The $GAD_{65/67}$ antibody used detected a band doublet at 65 and 67 kDa in the positive control lanes (Fig. 3-4). HT-22 cell extracts were also positive for $GAD_{65/67}$, with bands running at the anticipated molecular weight sizes of 65 and 67 kDa (Fig. 3-4). Immunological detection of the presence of $GABA_A$ (α1-5 subunits) and $GABA_B$ receptor proteins by Western blotting was attempted with several different commercially

available antibodies. None of the purchased antibodies successfully labeled $GABA_A$ or $GABA_B$ receptor proteins from HT-22 cell homogenate or fresh homogenate from mouse hippocampus (positive control). As multiple assays were run, we concluded that the commercial antibodies did not possess high affinity for the antigens.

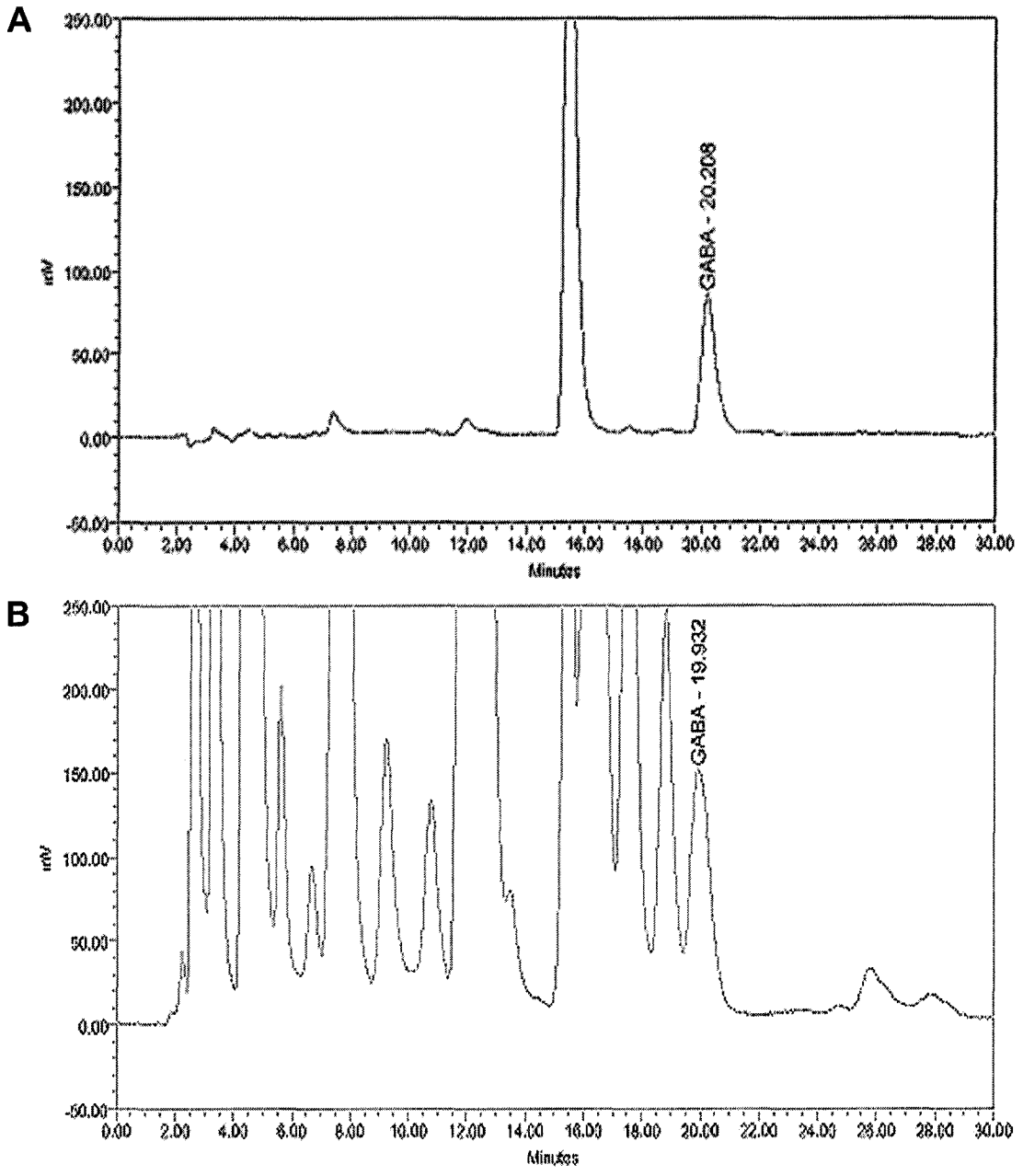

Figure 3-3 HPLC analysis of HT-22 cells.

Panel A displays a representative chromatograph obtained from a GABA standard dissolved in methanol mixed with fluoroaldehyde reagent (see Materials and Methods for details). Panel B displays a representative chromatograph obtained from HT-22 cell lysates prepared in methanol mixed with fluoroaldehyde reagent.

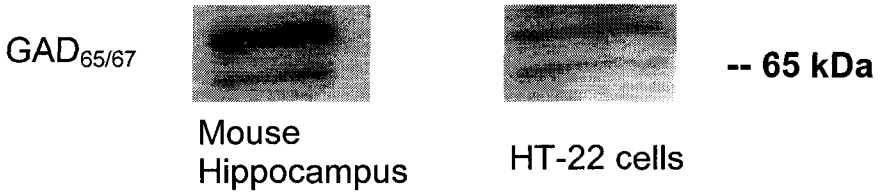

Figure 3-4 Western blotting analysis of $GAD_{65/67}$ in HT-22 cells.

The $GAD_{65/67}$ proteins were visualized by Western blotting using anti-$GAD_{65/67}$ antibody. Expected protein size for each protein are 65 and 67 kDa for GAD_{65} and GAD_{67}, respectively. Mouse hippocampus homogenate was used as a positive control for $GAD_{65/67}$ immunoreactivity.

To investigate whether HT-22 cells possess GABA-T, an assay to determine activity levels of GABA-T was performed. Results showed that HT-22 cells did not exhibit GABA-T activity. As antibodies that recognize GABA-T protein are not available, RT-PCR was used to detect mRNA for GABA-T. Analyses showed that in HT-22 cells, no GABA-T-specific mRNA was available for amplification (Fig. 3-5).

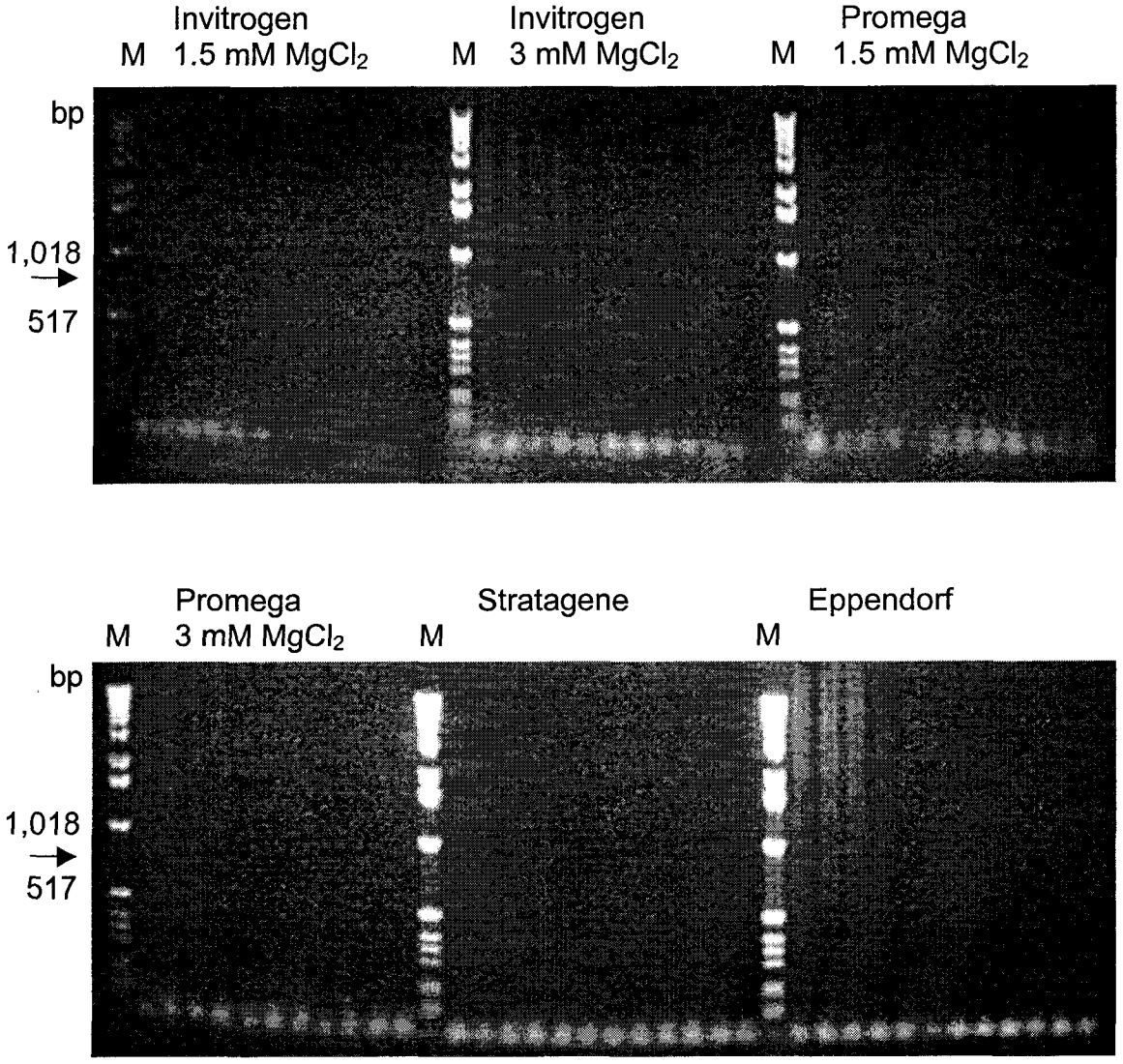

Figure 3-5 GABA-T RT-PCR.

RT-PCR for GABA-T mRNA was performed using several commercially available kits (Invitrogen, Stratagene, Promega and Eppendorf). $MgCl_2$ was added to Invitrogen and Promega kits to 1.5 or 3 mM final concentrations. The expected band size was 873 bp (indicated by an arrow). M; 1 kb DNA ladder marker.

3.3 Effect of PLZ, PEH and NAP on HT-22 cells under glutamate toxicity

3.3.1 Cytotoxic effect of glutamate

The degree to which glutamate can induce cytotoxicity in HT-22 cells was examined. Glu was added to the cell culture medium at a final concentration of 2, 5 or 10 mM and the cells incubated for 24 hours. At the end of the 24 hour incubation, the cell viability was assessed with the MTT assay. Results showed that Glu significantly reduced the cell viability by approximately 40% and 80% in the media containing 5 and 10 mM, respectively. Although incubation with 2 mM Glu showed a trend toward decreasing cell viability, it did not reach statistical significance (Fig. 3-6). Consequently, 5 and 10 mM Glu concentrations were chosen to study the potential neuroprotective properties of PLZ, PEH and NAP under Glu cytotoxicity conditions.

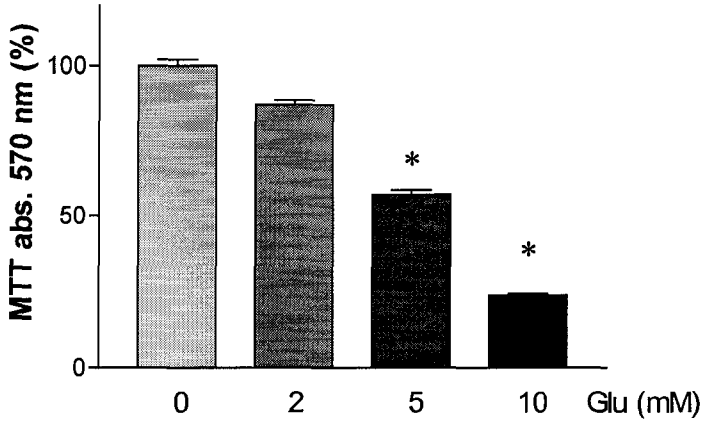

Figure 3-6 Dose dependent Glu cytotoxicity on HT-22 cells.

HT-22 cells were incubated with varying concentrations of Glu for 24 hours and the cell viability was measured by MTT assay. The cell viability of control cells (Glu 0 treated group) was shown as 100 %. * denotes significant difference ($P < 0.05$) in the cell viability compared to the control (Cont) group. Experiments were repeated 5 times.

3.3.2 The effect of PLZ on HT-22 cell viability

HT-22 cells were incubated for 24 hours in the presence of a wide range of concentrations of PLZ and the cell viability was determined by the MTT assay at the end of the incubation period. At the highest concentration (100 μM) of PLZ tested, HT-22 cell viability showed a trend toward a decrease, but the difference did not reach statistical significance for this, or any, of the 0 -100 μM concentration range evaluated.

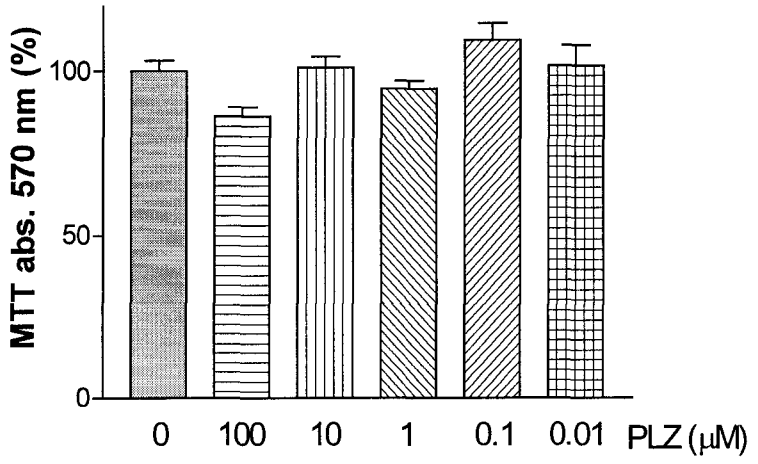

Figure 3-7 The effect of PLZ on HT-22 cell viability.

HT-22 cells were incubated with varying concentrations of PLZ for 24 hours and the cell viability was measured by MTT assay. The cell viability of control cells (no PLZ) was shown as 100%. Experiments were repeated 5 times.

3.3.3 Neuroprotective effects of PLZ

HT-22 cells were co-incubated with 5 mM Glu and several concentrations (0.01-100 μM) of PLZ for 24 hours after an hour preincubation with PLZ. Results showed that 5 mM Glu decreased cell viability by 50% as observed earlier, and

that none of the concentrations of PLZ tested significantly increased cell viability (Fig. 3-8). However, in cells incubated with 100 μM PLZ and 10 mM Glu, significant neuroprotection was observed (Fig. 3-9). Specifically, incubation with 10 mM Glu alone reduced HT-22 cell viability to approximately 25% to that of control conditions. After co-incubation with 100 μM PLZ, the cell viability was increased to 70% of that of control conditions. No other PLZ concentration showed any neuroprotective properties.

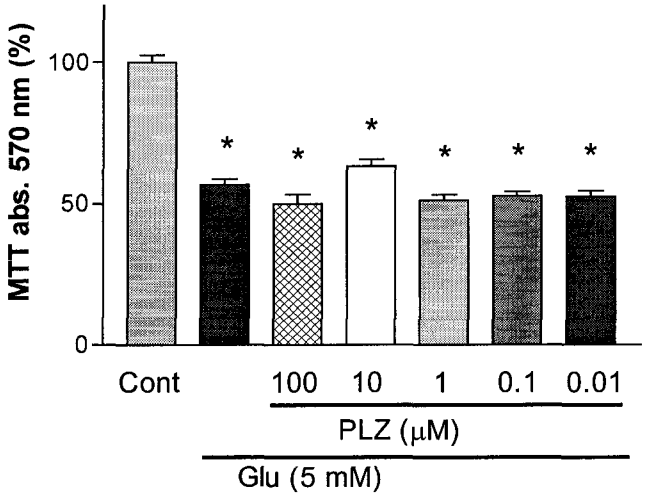

Figure 3-8 PLZ did not rescue HT-22 cells from 5 mM Glu cytotoxicity.

HT-22 cells were preincubated for 1 hour with one of varying concentrations of PLZ followed by a 24-hour incubation of PLZ plus 5 mM Glu. * denotes significant difference ($P < 0.05$) in the cell viability compared to the control (Cont) group. Experiments were repeated 6 times.

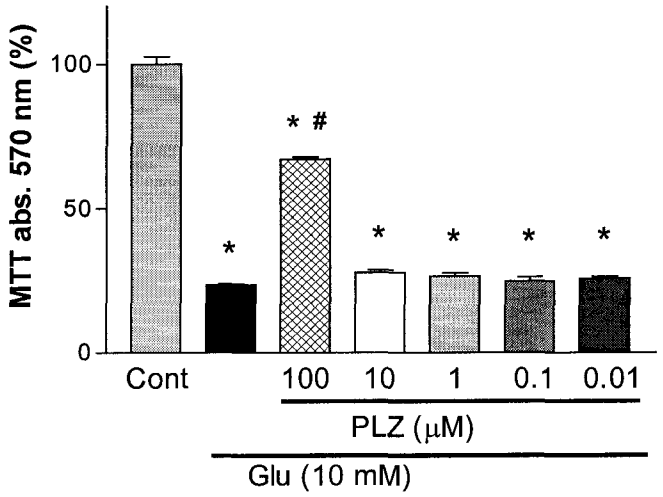

Figure 3-9 PLZ rescued HT-22 cells from 10 mM Glu cytotoxicity.

HT-22 cells were incubated with 10 mM Glu with indicated concentrations of PLZ for 24 hours following one hour preincubation with corresponding PLZ concentration. * denotes significant difference ($P< 0.05$) in the cell viability compared to the control (Cont) group and # denotes significant difference ($P<0.05$) compared to the Glu treated group. Experiments were repeated 6 times.

3.3.4 Effect of increased recovery time on cell viability

The MTT assay used in these investigations assesses the cell viability from the accumulation of insoluble formazan salt dye, which is generated by the mitochondria from the conversion of the water-soluble tetrazolium salt. In other words, the assay measures mitochondrial activity. Although the cell viability assessed by MTT assay and trypan blue staining were observed to correlate (data not shown) and have been reported to correlate after a 24-hr incubation with Glu (Davis and Maher, 1994), HT-22 cells could be either dead, dying or surviving with a low mitochondrial activity. To clarify whether HT-22 cells were dead, dying or protected by PLZ after the initial 24-hr incubation with Glu, the

cells were coincubated with PLZ and Glu containing medium for 24-hr, then the medium was replaced with fresh medium without Glu and PLZ and the cells were incubated for further 24-hr period. The results, displayed in Fig. 3-10A, showed that under a 5 mM Glu cytotoxic condition, PLZ, at any of the concentrations tested, did not induce any neuroprotection. However, the neuroprotective effect of 100 μM PLZ from 10 mM Glu-induced toxicity was maintained while all other concentrations of PLZ tested showed no significant effect (Fig. 3-10B).

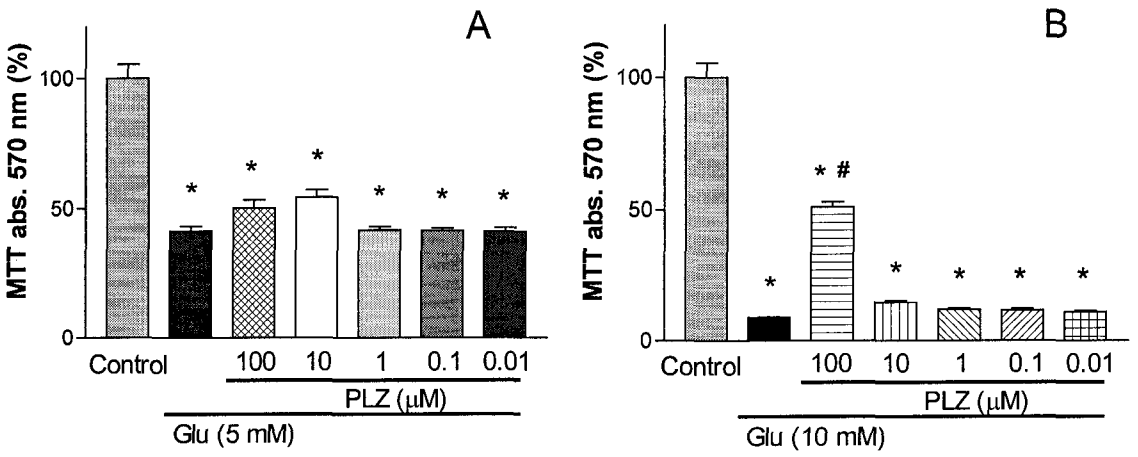

Figure 3-10 Assessment of the neurorescue properties of PLZ at 48 hours after Glu cytotoxicity.

HT-22 cells were incubated for 24 hours in fresh media after the initial 24 hour 5 mM (panel A) or 10 mM (panel B) Glu plus PLZ co-treatment. * denotes significant difference ($P < 0.05$) in the cell viability compared to the control (Cont) group and # denotes significant difference ($P<0.05$) compared to the Glu treated group. Experiments were repeated 6 times.

3.3.5 Determination of the optimal concentration of PLZ for neuroprotection

To better elucidate the concentration of PLZ which can optimally protect HT-22 cells from Glu toxicity, HT-22 cells were incubated in the presence of both Glu and a more focussed range of PLZ concentrations. PLZ is soluble in water; therefore it is possible to prepare a medium that contains relatively high concentrations of PLZ. PLZ was dissolved in medium containing 0.01% DMSO (to produce conditions consistent with those described in section 3.3.2-4) to a concentration range between 320 μM and 10 μM. At the highest concentration of PLZ (320 μM), cell viability was significantly reduced to approximately 75% of non-treated cells (Fig. 3-11). The optimal protection from 10 mM Glu cytotoxicity was observed at 180 and 100 μM PLZ concentrations (Fig. 3-12). Hence, the following experiments aimed at investigating the mechanism by which PLZ protects HT-22 cells from Glu toxicity (in section 3.4) were carried out using 100 μM PLZ and 10 mM Glu.

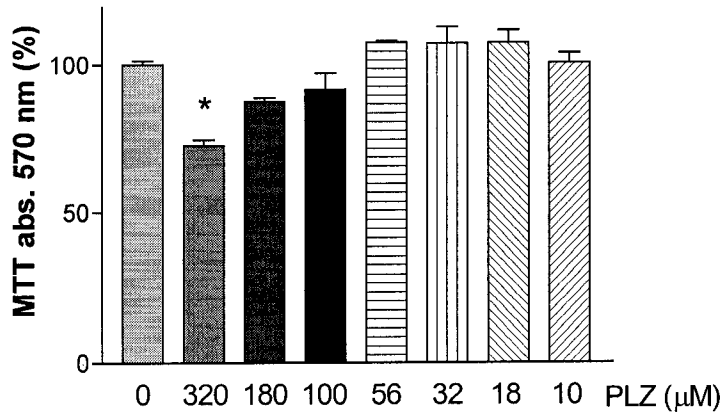

Figure 3-11 Dose response effect of PLZ on HT-22 cell viability.

HT-22 cells were incubated with various concentrations of PLZ for 24 hours. * denotes significant difference (P< 0.05) in the cell viability compared to the control (Cont) group. Experiments were repeated 5 times.

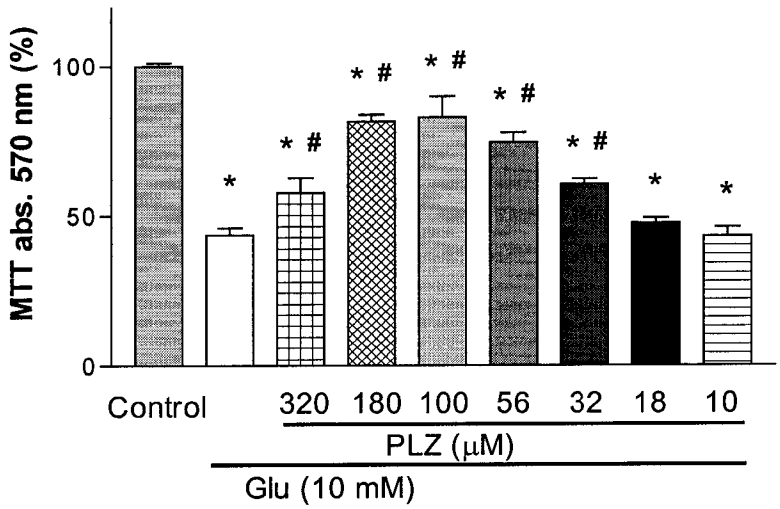

Figure 3-12 Dose response effect of PLZ on HT-22 cells with 10 mM Glu treatment.

HT-22 cells were incubated for 24 hour with 10 mM Glu plus various concentrations of PLZ following a one hour preincubation with the corresponding PLZ concentration. * denotes significant difference (P< 0.05) in the cell viability compared to the control (Cont) group and # denotes significant difference (P<0.05) compared to the Glu treated group. Experiments were repeated 6 times.

3.3.6 Effect of PEH on HT-22 cell viability

Working solutions of PEH were obtained by diluting a 1 M stock solution in the cell culture medium to a maximum concentration of 0.01% (v/v) DMSO. DMSO is toxic to the cells at high concentration, but 0.01 % (v/v) DMSO in cell culture medium did not induce cell toxicity (data not shown). Therefore, the highest concentration of PEH was limited to 100 μM (0.01% of 1 M stock solution) in the medium. This concentration was relevant to the concentrations used in *in vivo* studies which showed that PLZ and PEH protected neurons from global ischemia induced in gerbils at a dose of 30 mg (220 μmol)/kg (Todd et al., 1999). The average total blood volume of a gerbil is estimated to correspond to approximately 7% of its body weight. Therefore, assuming that the distribution of PLZ in the blood was consistent and metabolism of PLZ did not occur, the approximate concentration in the blood of PEH injected to gerbils in the Todd et al. (1999) study was calculated as approximately 3.14 mM, which was well above the concentration used in this thesis.

PEH is a putative metabolite of PLZ. While PLZ possesses both GABA-T and MAO inhibitory effects, PEH has GABA-T inhibitory activity (Parent et al., 2002) and weak MAO inhibitory (MAOI) activity (personal communication, Dr. Baker, University of Alberta, AB, Canada). As shown earlier, GABA-T was not detected in HT-22 cells. Therefore, examining the neuroprotective properties of PEH would help to clarify the importance of MAO-inhibiting activity of PLZ in protecting HT-22 cells from oxidative stress.

To determine whether PEH itself affects HT-22 cell viability, a wide range (100-0.01 μM) of PEH concentrations were incubated with HT-22 cells for 24 hours and the cell viability was determined by the MTT assay at the end of the 24-hr incubation period. Results showed that no concentration of PEH altered HT-22 cell viability compared to the non-PEH treated group (Fig. 3-13).

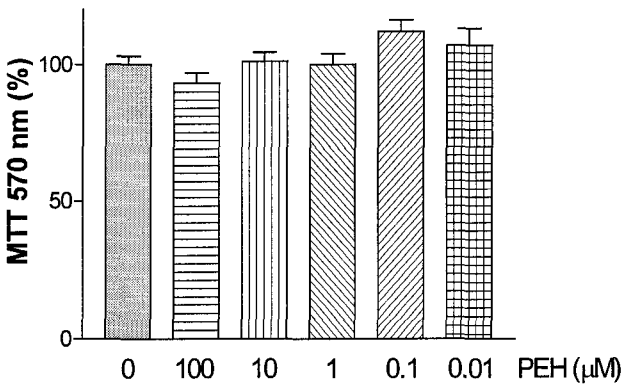

Figure 3-13 Dose response of PEH on HT-22 cell viability.

HT-22 cells were incubated with indicated concentration of PEH for 24 hours and the cell viability was measured by MTT assay. The cell viability of control cells (no PEH) is shown as 100 %. Experiments were repeated 5 times.

3.3.7 PEH did not protect neurons from glutamate cytotoxicity

HT-22 cells were co-incubated with 5 mM Glu and several concentrations (0.01-100 μM) of PEH for 24 hours after an hour preincubation with PEH. None of the PEH concentrations tested affected the toxicity induced by 5 mM Glu toxicity on HT-22 cells (Fig. 3-14A). Interestingly, co-incubation of 10 μM PEH with 10 mM Glu not only lacked protecting effects from Glu toxicity, but this combination appeared to exacerbate cell death (Fig. 3-14B).

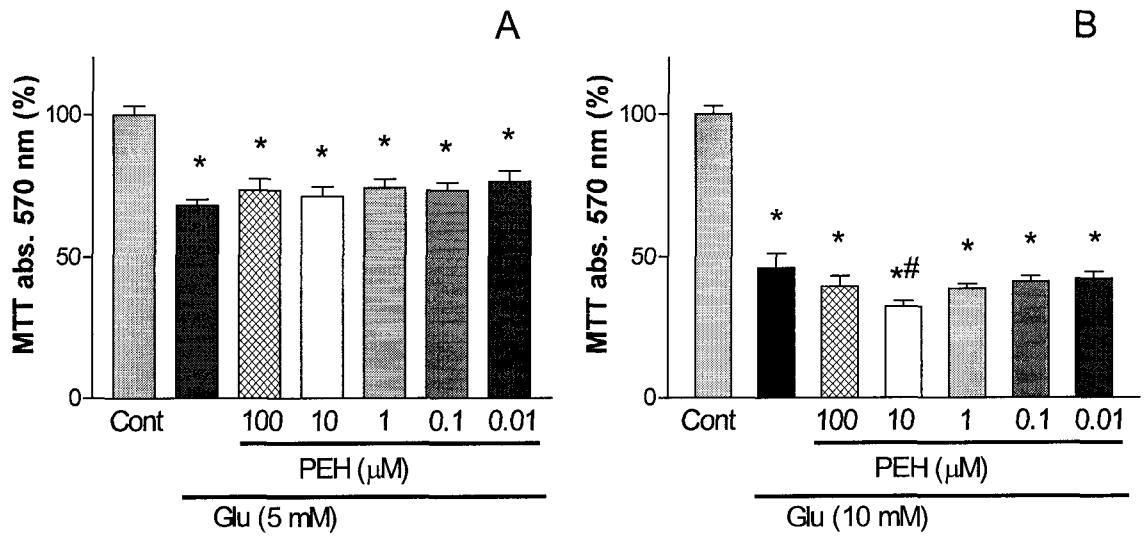

Figure 3-14 Dose response effects of PEH on 5 mM and 10 mM Glu-induced cytotoxicity.

HT-22 cells were incubated with either 5 mM (panel A) or 10 mM (panel B) Glu with indicated concentrations of PEH for 24 hours following one hour preincubation with corresponding PEH concentration. * denotes significant difference ($P< 0.05$) in the cell viability compared to the control (Cont) group and # denotes significant difference ($P<0.05$) compared to the Glu-treated group. Experiments were repeated 6 times.

3.3.8 Effect of increased recovery time on cell viability

Although PEH failed to demonstrate any initial improvement in neuronal cell viability under Glu cytotoxic conditions, it was hypothesized that PEH might offer a delayed protective effect. To verify whether HT-22 cells are dead/dying or that PEH could exert a delayed protection beyond the initial 24 hour incubation with Glu, HT-22 cells were cultured in fresh medium without Glu or PEH for an additional 24 hours post the initial 24 hour co-incubation. Fig. 3-16a showed that under 5 mM or 10 mM Glu cytotoxic conditions, PEH did not increase the numbers of surviving neurons at any of the concentrations tested. The enhanced neuronal cell death observed after the initial 24 hour incubation period

with 10 μM PEH and 10 mM Glu remained after the additional 24 hour incubation with fresh medium (Fig. 3-16b).

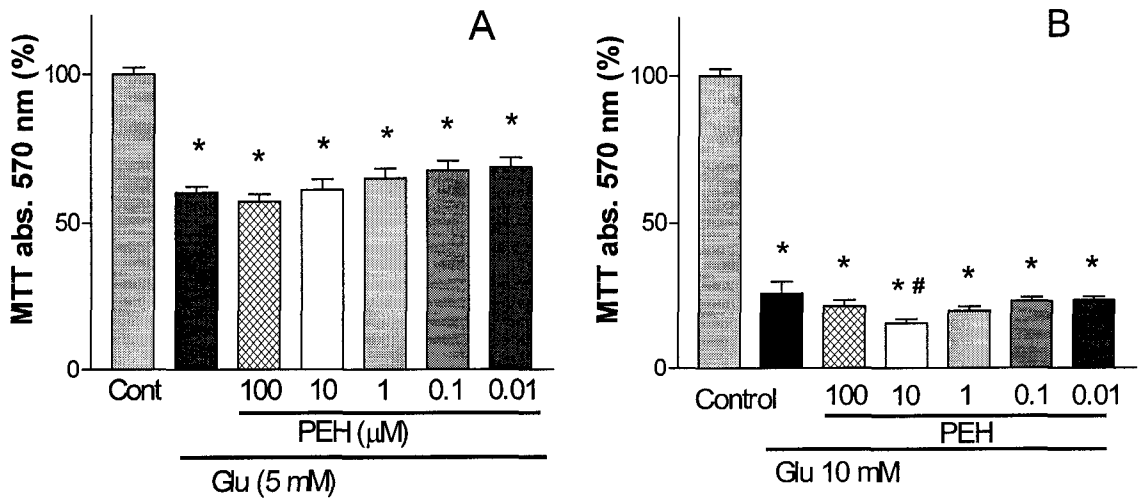

Figure 3-15 Assessment of PEH effect on HT-22 cells after 24 hour recovery period.

HT-22 cells were incubated for 24 hour in the presence of fresh media after the initial 24 hour 5 mM (panel A) or 10 mM (panel B) Glu plus PEH co-treatment. * denotes significant difference ($P < 0.05$) in the cell viability compared to the control (Cont) group and # denotes significant difference ($P<0.05$) compared to the Glu-treated group. Experiments were repeated 6 times.

3.3.9 Evaluation of PEH stability

As mentioned earlier, a 1 M stock solution of PEH was dissolved in DMSO and stored in aliquots at –20 °C until use to avoid repeated thaw-refreeze cycles. Because there was no previous study to investigate the consequences of PEH storage in diluted state in DMSO over prolonged periods, the possibility that the structure of PEH might have been compromised under such conditions could not be eliminated. Hence PEH breakdown could explain the lack of neuroprotective effect. To investigate this theory, gas chromatography (GC) analysis of PEH in

stock solution was performed with the technical assistance of Ms. G. Raul. Gas chromatography analysis showed that preservation of PEH at –20 °C as stock solution did not compromise its integrity as measured by the retention time of freshly dissolved PEH being identical to that of a freeze-thawed PEH stock solution (data not shown). Therefore, the stability of the PEH molecule was not altered through the preparation of stock solution and subsequent storage, and this confirmed that PEH did not protect HT-22 cells from Glu cytotoxicity despite being present in the culture medium.

3.3.10 The effect of NAP on H-22 cells

NAP is another putative metabolite of PLZ which has been shown to possess MAOI activity (McKenna et al., 1992). MAOI agents such as clorgyline and harmine have been shown to protect HT-22 cells from oxidative stress (Maher and Davis, 1996), PLZ's MAOI activity is thought to be important in the observed neuronal protection. However, PLZ has been reported to affect a wide range of enzymes (Holt et al., 2004). Because NAP possesses similar MAOI activity to PLZ, but lacks GABA-T inhibiting effects, we investigated whether it would have similar neuroprotective effects.

Initially, the effect of NAP on HT-22 cell viability was examined. HT-22 cells were incubated with wide range of concentrations of NAP (100 to 0.01 μM) for 24 hours. Results showed that none of the concentrations used had any significant effect on cell viability (Fig. 3-16).

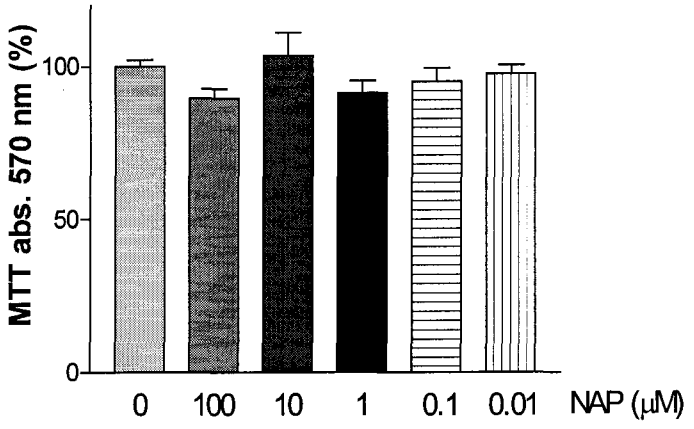

Figure 3-16 Dose response of NAP on HT-22 cell viability.

HT-22 cells were incubated with indicated concentrations of NAP for 24 hours and cell viability was measured by MTT assay. The cell viability of control cells (no NAP) was shown as 100 %. Experiments were repeated 5 times.

3.3.11 Effect of NAP on glutamate toxicity

HT-22 cells were incubated with 5 mM and 10 mM Glu and a wide range (100 to 0.01 μM) of NAP concentrations for 24 hours after an initial 1-hr preincubation with the corresponding NAP concentration. None of the concentrations tested significantly rescued HT-22 cells from 5 mM Glu cytotoxicity (Fig. 3-17A). However, 100 μM NAP treatment significantly protected HT-22 cells from the cytotoxicity induced by 10 mM Glu (Fig. 3-17B) and it is interesting to note that the degree of protection offered by NAP treatment was much less than that observed with PLZ treatment (Fig. 3-9). No other concentration of NAP showed any neuroprotective properties.

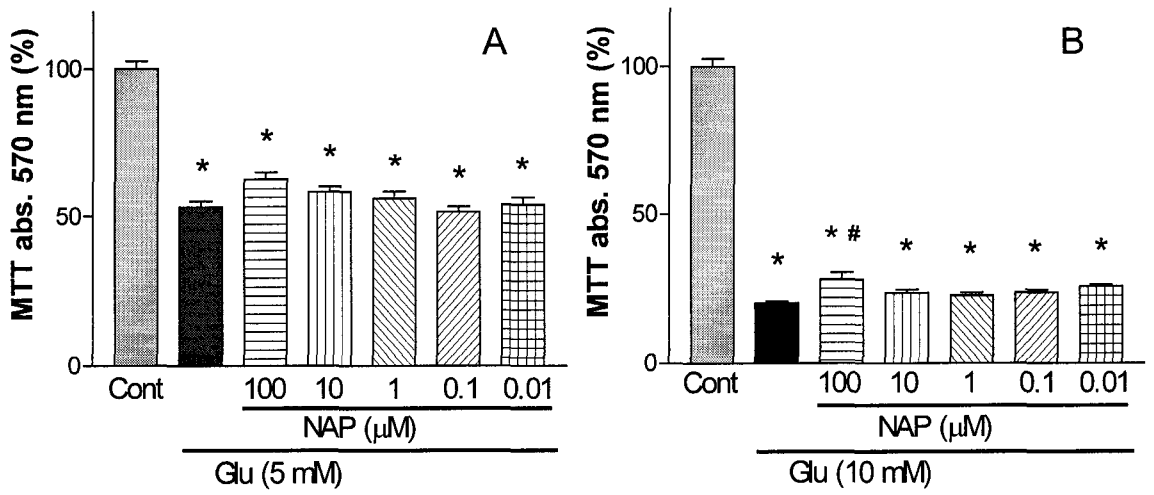

Figure 3-17 Dose response effects of NAP on 5 mM and 10 mM Glu cytotoxicity.

HT-22 cells were incubated with either 5 mM (panel A) or 10 mM (panel B) Glu with indicated concentration of NAP for 24 hours following one hour preincubation with corresponding NAP concentration. * denotes significant difference ($P< 0.05$) in the cell viability compared to the control (Cont) group and # denotes significant difference ($P<0.05$) compared to the Glu-treated group. Experiments were repeated 6 times.

3.3.12 Effect of increased recovery time on cell viability

As with PLZ and PEH, we evaluated whether NAP would show a delayed protective effect from Glu toxicity. To this end, HT-22 cells were incubated in fresh medium for an additional 24 hours following the initial 24 hour co-incubation with Glu and NAP as described previously. The results showed that 100 μM NAP demonstrated significant improvement of cell viability in cultures treated with 5 mM Glu compared to cells treated with just Glu (Fig. 3-18A). This neuroprotective effect was not observed in the previous experiment where the viability assay was performed after the 24 hour incubation with Glu and NAP (Fig. 3-17). With regard to the cultures exposed to 10 mM Glu, none of the

concentrations of NAP tested improved cell viability after the additional 24 hour fresh media incubation period (Fig. 3-18B).

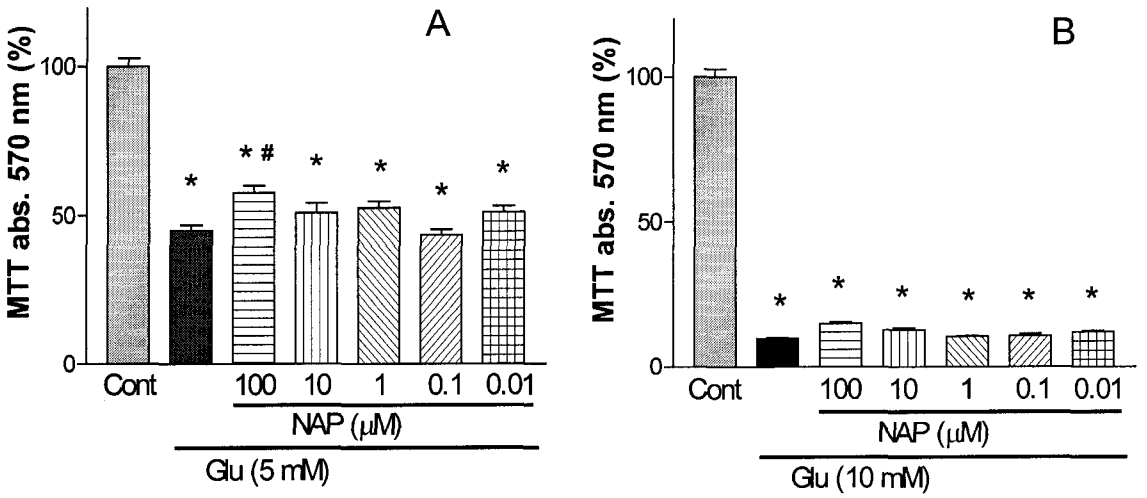

Figure 3-18 Assessment of NAP effect on HT-22 cells after 24 hour recovery period.

HT-22 cells were incubated for 24 hour in the presence of fresh media after the initial 24 hour 5 mM (panel A) or 10 mM (panel B) Glu plus NAP co-treatment. * denotes significant difference ($P < 0.05$) in the cell viability compared to the control (Cont) group and # denotes significant difference ($P<0.05$) compared to the Glu treated group.

3.3.13 Determination of optimal NAP concentration for the neuroprotection from glutamate toxicity

McKenna et al. (1996) reported that NAP has significantly lower MAOI activity than PLZ. Specifically, when NAP or PLZ were added to rat brain homogenate, PLZ showed more than 95 % inhibition of MAO activity at a dose of 0.05 mmol/kg animal weight while NAP required a much higher concentration 0.2 mmol/kg animal weight to inhibit MAO to the same degree. This and other reports suggest that drugs that inhibit MAO are also neuroprotective and the likely mechanism is

through a reduction in oxidative stress (Maher and Davis, 1996). Thus, it was possible that at higher concentrations, NAP may show a better neuroprotective effect.

To evaluate a dose-response effect of relatively high concentrations of NAP on cell viability, HT-22 cells were incubated with an expanded range of concentrations of NAP for 24 hours. The results showed that the highest concentration of NAP used, 320 μM significantly decreased cell viability while all other concentrations tested had no effect on the cell viability (Fig. 3-19A). A concentration of 100 μM was shown to be optimal for protecting HT-22 cells from cytotoxicity induced by 10 mM Glu (Fig. 3-19B).

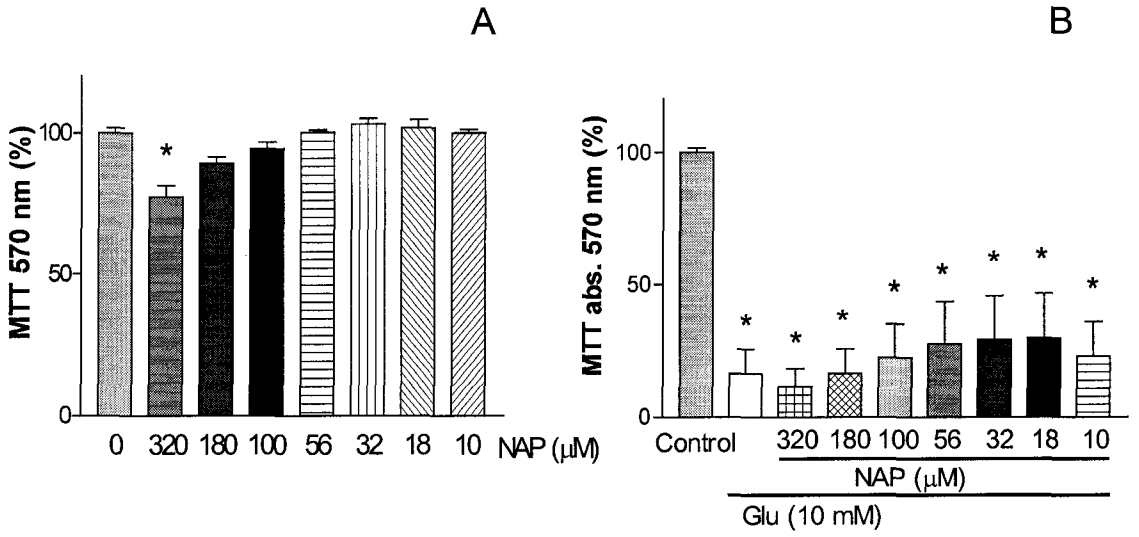

Figure 3-19 Dose response effect of NAP on HT-22 cells.

Panel A: HT-22 cells were incubated with various concentrations of NAP for 24 hours. Panel B: HT-22 cells were incubated for 24 hour with 10 mM Glu plus various concentrations of NAP following to one hour preincubation with corresponding NAP concentration. * denotes significant difference ($P < 0.05$) in the cell viability compared to the control (Cont) group and # denotes significant difference ($P<0.05$) compared to the Glu treated group. Experiments were repeated at least 5 times.

3.4 The mechanism of PLZ neuroprotection

3.4.1 Evaluation of PLZ as an ROS scavenger

The Glu cytotoxicity observed in HT-22 cells is due to oxidative stress as a result of a depletion of GSH and accumulation of ROS (Sagara et al., 1999). Whether PLZ protects HT-22 cells through a reduction of ROS, however, was inconclusive from prior results. Investigation of the ability of PLZ to protect neurons from the toxic effects of H_2O_2 was undertaken. First, the concentration of H_2O_2 necessary to induce cell death in HT-22 cells was determined by incubating cells with 10, 20 or 40 μM H_2O_2 for 24 hours. At concentrations of 20 and 40 μM H_2O_2, the cell viability was reduced by approximately 50% and 90%, respectively (Fig. 3-20). From these results, 20 μM H_2O_2 was selected for further experiments. Surprisingly, results showed that the co-incubation of PLZ with 20 μM H_2O_2 following a one hour preincubation with PLZ alone not only failed to protect HT-22 cells, but significantly decreased cell viability compared to 20 μM H_2O_2-treated cells (Fig. 3-21A). After a 24-hr recovery period with fresh medium following the initial 24-hr PLZ/H_2O_2 co-treatment, the cell viability did not improve (Fig. 3-21B).

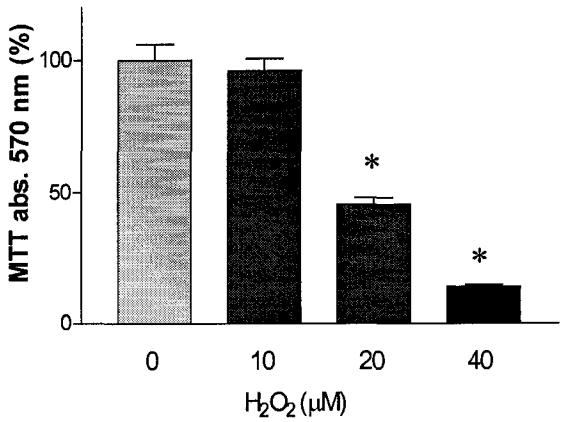

Figure 3-20 Dose response of H_2O_2.

HT-22 cells were incubated with 10, 20 or 40 μM H_2O_2 for 24 hours and the cell viabilities were measured by MTT assay. * denotes significant difference ($P< 0.05$) in the cell viability compared to the control (Cont) group. Experiments were repeated 4 times.

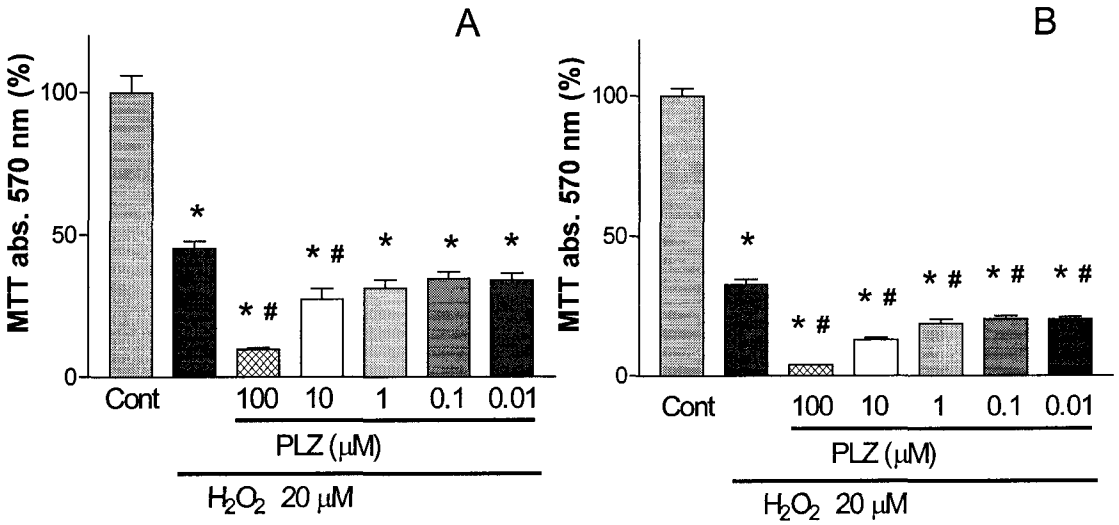

Figure 3-21 Dose response of PLZ effect under H_2O_2 toxicity.

Panel A: HT-22 cells were incubated in 20 μM H_2O_2 medium with or without PLZ for 24 hours following the preincubation. Panel B: HT-22 cells were incubated 24 hours in fresh medium for recovery, following to initial 24 hour co-incubation with H_2O_2 plus PLZ. * denotes significant difference ($P< 0.05$) in the cell viability compared to the control (Cont) group and # denotes significant difference ($P<0.05$) compared to the Glu treated group. Experiments were repeated 6 times.

3.4.2 Effect of PLZ on GSH levels

As mentioned previously, GSH is depleted in HT-22 cells under Glu toxicity (Davis and Maher, 1994). To determine whether the neuroprotective effect of PLZ was due to increased GSH levels, GSH was assayed after 1, 2, 4, 8 and 16 hr incubation with PLZ, Glu or PLZ+Glu. Results showed that after 24 hr incubation with 10 mM Glu, few cells were recovered after harvesting and centrifugation (data not shown), probably because most dead/damaged cells remained in the supernatant during centrifugation due to their smaller mass compared to healthy cells. Analyses showed that GSH levels were not significantly different between control (incubated with vehicle) and PLZ treated-groups at any time point (Fig. 3-22). The Glu and Glu+PLZ groups had lower GSH content compared to the other two groups after 2 hour incubation period. In HT-22 cells co-incubated with Glu + PLZ, the GSH levels were similar to those observed in the Glu treated cells for all time points except the 16 hour group where GSH levels were found to be significantly higher in the Glu + PLZ treated-cells compared to those treated with Glu alone.

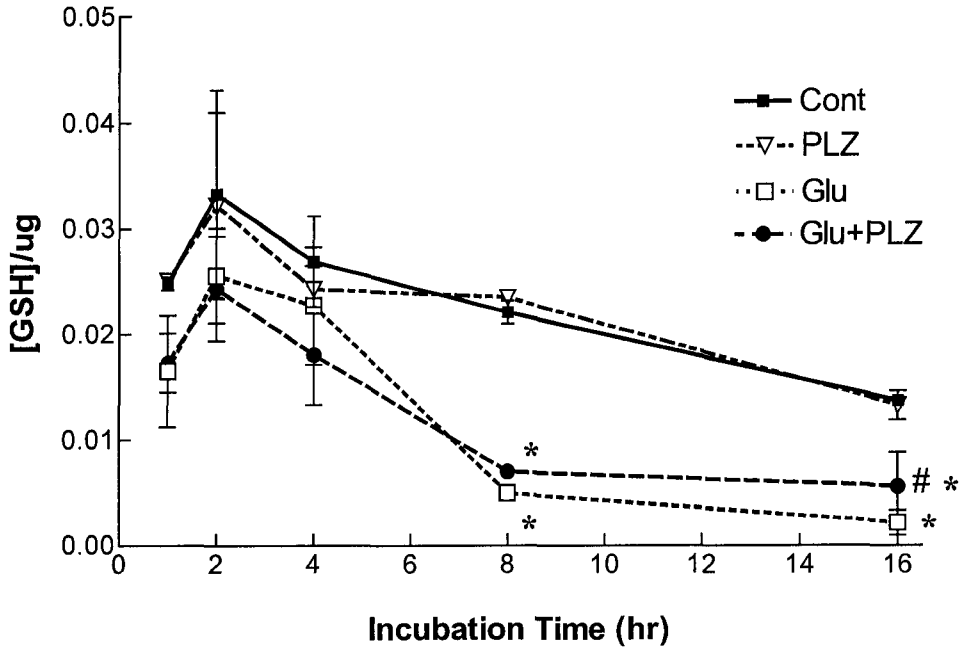

Figure 3-22 The concentration of GSH, corrected for protein content.

HT-22 cells were incubated with 10 mM Glu with or without 100 μM PLZ and harvested at 1, 2, 4, 8 and 16 hours following one hour preincubation with 100 μM PLZ . * denotes significant difference ($P< 0.05$) in the cell viability compared to the control (Cont) group and # denotes significant difference ($P<0.05$) compared to the Glu treated group. Each value represents an average value of at least 6 repeated experiments.

3.4.3 Bcl-xL levels in HT-22 cells during glutamate cytotoxicity

HT-22 cells subjected to Glu toxicity exhibit apoptotic features (Tan et al., 1998). The apoptotic pathway involves the activation/deactivation of pro-apoptotic proteins including the Bcl protein family members. The Bcl family contains both pro- and anti-apoptotic proteins such as Bcl-2 and Bcl-xL (anti-apoptotic), and Bax and Bak (pro-antiapototic). Overexpression of Bcl-xL has been reported to protect yeast from H_2O_2 induced cytotoxicity (Chen et al., 2003) and murine cell lines from GSH depletion (Bojes et al., 1997). Therefore, we sought to investigate whether PLZ can induce increased expression of Bcl-xL. HT-22 cells

were harvested at 1, 2, 4, 8, and 16 hours after the addition of 10 mM Glu to the medium and Western Blotting was performed to measure the amount of Bcl-xl protein present. To obtain an average change in Bcl-xl protein level, cell lysates were pooled by treatment groups (control, Glu, PLZ, and Glu plus PLZ, minimal n = 5). After a 16 hour incubation with Glu alone, a Bcl-xL protein amount change was visible (Fig. 3-23). It was therefore of interest to quantify the protein amount at that time point. The density of the Bcl-xL protein band was corrected using the actin immunoreactive band as an internal standard to control for protein loading. After correction of Bcl-xl amount with actin, it appeared that there was virtually no difference between the Glu-treated group and PLZ/Glu co-treated group, although those two groups did exhibit decreased Bcl-xL protein compared to the control and PLZ-treated groups (Fig. 3-24).

Western blotting analyses of caspase-3 and other Bcl family proteins did not yield conclusive results. Western blotting for caspase-3 required very high protein loading (~100 μg/lane) even from normal brain homogenates. However, no band was detected using an equal amount of proteins from HT-22 cells, although it may be that the amount of caspase-3 in the HT-22 cells was below detectable levels. Other Bcl family proteins such as Bcl-2, Bak, and Bad, as well as phosphorylated (activated) Bcl-2 and Bak were also not detectable in HT-22 cells. To investigate the quality of the antibodies, Western blots using rat and mouse brain homogenates were run. The antibodies failed to recognize the antigens in both mouse and rat brain homogenates which are known to contain all the antigens. Therefore the antigen recognition ability of the commercially

available antibodies was questionable. To date, there has been no other report regarding the existence of the caspase protein family and Bcl protein family in HT-22 cells. This project was the first to show that HT-22 cells express Bcl-xL protein.

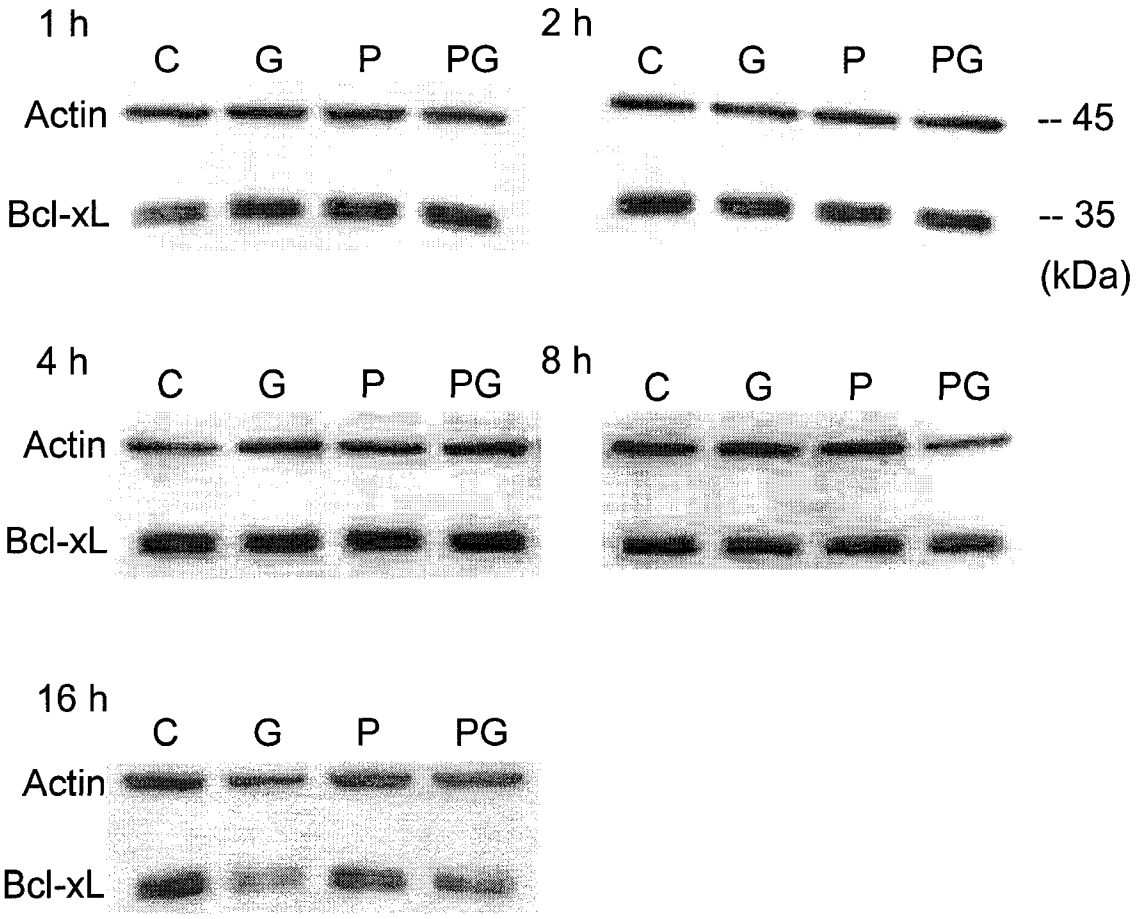

Figure 3-23 Bcl-xL protein level change over time

HT-22 cells were incubated with 10 mM Glu with or without co-incubation of 100 μM PLZ and harvested at indicated time points. Bcl-xL protein levels were visualized by Western blotting. C, control; G, Glu treated group; P, PLZ treated group; and PG, PLZ plus Glu treated group.

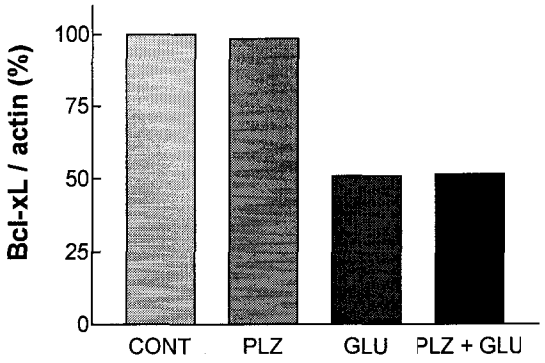

Figure 3-24 The Bcl-xL protein amount corrected by actin protein amount

The density of immunoreaction of Bcl-xL and actin of 16 hour incubated groups were assessed by MCID Elite 7.0 program. The Bcl-xL protein amount corrected by actin protein amount of intact (control) group was plotted as 100 %.

Chapter 4 Discussion

Cerebral ischemia (stroke) induces elevated secretion of Glu in the brain, which triggers both oxidative stress and excitotoxicity, ultimately leading to neuronal cell death (Braughler and Hall, 1989; Lipton, 1999). Oxidative stress is caused by accumulation of ROS in the cell. Mechanisms for ROS accumulation include increased generation of ROS and lowered activity of ROS scavenging systems. For example, accumulation of ROS can be caused by the depletion of the main ROS scavenger in neuronal cells, namely GSH (Murphy et al., 1989). ROS generation observed in the brain during and after cerebral ischemia is mainly due to MAO activity (Suzuki et al., 1995; Tadano et al., 1995). Oxidative stress also causes neuronal cell death in various neuropathologies including Alzheimer's and Parkinson's diseases (Klein and Ackerman, 2003; Lev et al., 2003). Considering the detrimental impact of stroke, Alzheimer's and other neuropathologies on our society, it is important to find a model to study oxidative stress. HT-22 cells used in this thesis could provide a good model to study oxidative stress without the confounding effects of excitotoxic mechanisms because the cells lack Glu receptors (Davis and Maher, 1994).

4.1 GABAergic properties of HT-22 cells

Some of physiological and pharmacological characteristics of HT-22 cells have been previously studied and results showed that they do not express Glu receptors (Davis and Maher, 1994) nor estrogen receptors (Behl et al., 1995).

However, to date, there have been no reports regarding their GABAergic properties. The present study was the first of its kind to show that HT-22 cells contain GABA and express the GABA synthesizing enzymes, $GAD_{65/67}$. GABA was also detected in the cell culture media, suggesting that HT-22 cells possess mechanisms to secrete GABA. These findings and the fact that these cells lack Glu receptors, imply that HT-22 cells may have been derived from GABAergic neuronal cells, although it is possible that these characteristics were derived during the immortalizing process.

It is important to note that the presence of GABA receptors on the surface of HT-22 cells remains unknown. If HT-22 cells express GABA receptors, these cells would be a useful model to study the effects of GABA during oxidative stress. Administration of GABA, GABA site agonists, and $GABA_A$ receptor positive modulators have been shown to rescue neuronal cells from ischemic damage (Schwartz-Bloom and Sah, 2001). Moreover, administration of either PLZ or PEH has significantly rescued neuronal cells in a gerbil transient forebrain ischemic model (Todd et al., 1999). Since ischemia triggers both Glu receptor dependent excitotoxicity and Glu receptor-independent oxidative stress, it is unclear if an elevation in GABA levels combined with the GABA-T inhibition provided by those drugs would be effective to protect neuronal cell death from oxidative stress. Importantly, HT-22 cells do not express GABA-T mRNA nor possess GABA-T activity that can be detected.

4.2 PLZ and neuroprotection of HT-22 cells

Inhibitory effects of PLZ on both MAO and GABA-T have been reported in both *in vitro* and *in vivo* models (Baker et al., 1991). HT-22 cells were protected from oxidative stress after the administration of MAOIs such as clorgyline and lazabemide (Suzuki et al., 1995). Therefore, it was anticipated that PLZ would demonstrate a neuroprotective effect that could be attributed to its MAOI activity. Indeed, 100 μM PLZ significantly protected HT-22 cells from 10 mM Glu cytotoxicity, but lower PLZ concentrations tested did not.

In addition, it was rather surprising that PLZ did not show any neuroprotective effect from 5 mM Glu toxicity at any of the concentrations tested. This suggests that the Glu cytotoxicity mechanism could involve several different pathways. Five mM Glu treatment may trigger one cell death pathway while 10 mM Glu may trigger a completely different cell death creating a type of synergistic effect. Thus, PLZ likely only protects HT-22 cells from the death pathway(s) triggered by 10 mM Glu treatment as evidenced by similar cell viability levels cell in the 100 μM PLZ plus 10 mM Glu treatment group (~60%) and 5 mM Glu treatment group (~55%).

4.3 PEH and the neuroprotection of HT-22 cells

Injection of PEH into gerbils, in which transient forebrain ischemia was modeled, significantly rescued neurons of the hippocampal CA1 region (Todd et al., 1999). PEH is a metabolite of PLZ, and it possesses GABA-T inhibitory activity similar to

that of PLZ (Parent et al., 2002), and it has been shown to have only weak MAOI activity (Dr. Baker, University of Alberta, Edmonton, Canada, personal communication). Hence, PEH treatment of HT-22 cells under oxidative stress should clarify the importance of MAO inhibition activity of PLZ for its neuroprotective properties. PEH did not protect HT-22 cells from oxidative stress induced by either 5 mM or 10 mM Glu, thereby suggesting that MAOI activity of PLZ probably plays a vital role in neuroprotection from oxidative stress.

As GABA-T was not detected by either an enzymatic activity assay or RT-PCR methods, it is likely that the GABA-T inhibition activity of PLZ did not play a role in the promotion of HT-22 cell viability.

4.4 NAP and the neuroprotection of HT-22 cells

NAP is an acetylated form of PLZ (Mozayani et al., 1988). 100 μM NAP significantly protected HT-22 cells from 10 mM Glu toxicity at a concentration at which PLZ also showed significant neuroprotection, although the degree of neuroprotection provided by 100 μM PLZ was much greater than that of 100 μM NAP. Both NAP and PLZ inhibit MAO activity (McKenna et al., 1991). As mentioned earlier, MAOI activity is postulated to participate to the protection of HT-22 cells from oxidative stress induced by Glu treatment. Comparison of the MAOI activity of NAP and PLZ in rat brain homogenates revealed that 0.05 mmol/kg of NAP provided 40.5 % inhibition of MAO-A and 21.3% inhibition of MAO-B compared to the same dose of PLZ showing 97.9% inhibition of MAO-A, 70.8% inhibition of MAO-B. A higher dose of NAP (0.20 mmol/kg) showed a

similar degree of MAOI activity compared to PLZ (94.9% compared to 97.8% for MAO-A, and 79.6% relative to 87.2% for MAO-B, respectively). NAP did not, however, present the same degree of neuroprotective properties as PLZ even at the higher concentrations tested in this study. This may reflect the lower solubility of NAP than PLZ. For example, the original attempt to prepare 10 M NAP in DMSO resulted in the precipitation of NAP. Although 5 M NAP or lower concentrations in DMSO did not leave any visual clues of precipitated NAP, NAP may have a lower solubility when compared to PLZ solubility. Another possibility is that PLZ neuroprotection could be mediated by another mechanism other than MAOI activity. Indeed, Holt et al. (2004) postulated that PLZ can interact with many enzymes beside MAO. Some of those enzymes might be able to enhance protection of neuronal cells from oxidative stress, but these protective mechanisms were lost during the acetylation of PLZ to produce NAP.

4.5 Possible neuroprotective mechanism for PLZ

4.5.1 GSH

The cellular mechanisms functional during oxidative stress in HT-22 cells have been well documented and include the depletion in GSH and the accumulation of ROS species (Davis and Maher, 1994). Hence, whether cellular GSH amounts are affected by PLZ treatment was investigated. There was a small, but significant increase in GSH levels after 16 h co-incubation with Glu and PLZ compared to the Glu-treated group. Interestingly, however, there was no

significant difference in GSH amount between the two groups at earlier time points (1, 2, 4, and 8 h). This difference at 16 h could reflect lower production levels of ROS by the inhibition of MAO by PLZ over time or these results may be due to a different mechanism, such as an increase in GSH production or activity.

Sagara et al. (1998) created Glu toxicity-resistant HT-22 subclones by maintaining HT-22 cells in 10 mM Glu containing medium for two months and selecting for live cells. Glu resistant HT-22 subclones had higher resistance to cystine starvation, which ultimately inhibited the new production of GSH and depletion of GSH induced by administration of buthionine-[*S,R*]-sulfoximine (BSO) (Dargusch and Schubert, 2002). Additionally, the Glu toxicity-resistant HT-22 subclones were resistant to high concentrations of H_2O_2. The EC_{50} of H_2O_2 toxicity in parental HT-22 cells was 20 μM whereas in subcloned HT-22 cells it was 200 μM. The activities of GSH synthetase, GSH reductase and GSH-S-transferase were elevated in the study suggesting that Glu toxicity-resistant cells can produce, recycle, and upregurate the activity of GSH. To investigate whether PLZ increased cell resistance against ROS, HT-22 cells were incubated with H_2O_2 (the major ROS species in the cell) with or without co-treatment with PLZ.

Interestingly, HT-22 cells treated only with PLZ did not show an increase in GSH levels. This may imply that Glu treatment of HT-22 cells stimulates ROS production. The levels of intracellular ROS after treatment with MAOI agents such as clogyline did not differ between intact and Glu treated HT-22 cells (Maher and Davis, 1996). Moreover, the treatment with monoamine uptake

inhibitors, which did not affect intracellular H_2O_2 levels in intact HT-22 cells, showed a neuroprotective effects against Glu toxicity (Maher and Davis, 1996) suggesting that the increase in ROS production induced by Glu treatment may be due to monoamine uptake increase.

4.5.2 ROS

After 16 hour of PLZ and Glu co-treatment, GSH amounts in HT-22 cells increased significantly. Higher GSH levels can be attained if PLZ up-regulated cellular GSH activity by increasing its synthesis, increasing its activity and/or increasing its recycling, or if PLZ had ROS scavenging effects. In order to investigate the neuroprotective effect of PLZ on existing ROS levels, HT-22 cells were exposed to H_2O_2, which is a common intracellular ROS species generated by MAO metabolic activity. Surprisingly, PLZ not only failed to protect HT-22 cells from H_2O_2 toxicity, but it promoted such toxicity. Such unexpected results may be due to the complex effects PLZ has on a number of enzymes (Holt et al., 2004). Although neuronal cells have low catalase activity to metabolize H_2O_2, the inhibition of this enzyme might amplify the damage to cells. One hypothesis is that PLZ treatment may inhibit intracellular catalase activity so that H_2O_2 cytotoxicity is enhanced. To study the mechanism by which PLZ could amplify H_2O_2 toxicity, intracellular ROS levels could be compared between intact and PLZ treated cells with H_2O_2 treatment. In this case, PLZ did not improve the cell viability under H_2O_2 cytotoxicity suggesting that treating HT-22 cells with PLZ does not improve cell resistance to existing ROS. Therefore, PLZ might increase

the amount of GSH amount or its activity but has little ROS scavenging activity. However, it is more likely that lower production of ROS is responsible for the neuroprotective effects provided by PLZ.

4.5.3 Inhibitor of Apoptosis

Oxidative stress presents with both necrotic and apoptotic characteristics (Tan et al., 1998). Although HT-22 cells exposed to oxidative stress do not exhibit typical apoptotic DNA fragmentation, the cell death pathway does require protein synthesis to proceed through the conventional apoptotic pathway. One of the proteins involved in the apoptotic pathway is Bcl-xL. Bcl-xL is an anti-apoptotic protein as its activation is known to prevent apoptosis. Overexpression of Bcl-xL in yeast and mammalian cells induced higher resistance to oxidative stress (Bojes et al., 1997; Chen et al., 2003). Neuroprotection provided by PLZ, therefore, might involve the upregulation of Bcl-xL. To examine this hypothesis, HT-22 cells were harvested at 1, 2, 4, 8 and 16 hours of PLZ-Glu co-treatment. At 16 hours, the density of Bcl-xL protein immunoreacted band in Glu-treated cells was approximately half of those of intact and PLZ-treated cells. However, the Bcl-xL in Glu- and PLZ-co-treated cells was also lowered to the same level in Glu-treated cells. The results suggest that Bcl-xL is probably not involved in the neuroprotection induced by PLZ administration. The involvement of other Bcl family members, such as Bcl-2, Bak and Bad, remains unknown as the commercially available antibodies did not exhibit specificity toward mouse proteins (data not shown).

It has been suggested that caspases, the final effectors of the apoptosis pathway, may be triggered in the HT-22 cells responding to oxidative stress. The administration of the caspase-1 inhibitor, YVADfmk significantly reduced the number of dead HT-22 cells induced by Glu cytotoxicity (Dargusch and Schubert, 2002). However, caspase-1 is believed to activate proinflammatory cytokines, and it may not be directly involved in the apoptotic pathway. Caspase-3, on the other hand, has been clearly shown to play a part in the apoptotic pathway and the presence of cleaved and active form of caspase-3 is an indication that apoptosis is proceeding. In a project described in this thesis, Western blotting analysis for cleaved caspase-3 in HT-22 cells was undertaken to determine whether caspase-3 is involved in the cell death mechanism activated by Glu cytotoxicity. Cleaved caspase-3, however, was not detected in Western blotting analysis (data not shown). Other results in our lab from rat brain homogenates indicated that high protein amounts (~100 μg/lane) are required to detect caspase-3 by Western blotting (data not shown), and this requirement may be even higher for caspase-3 in HT-22 cells extracts to positively react. Alternatively, Tan et al. (1998) reported that the administration of a caspase-3 inhibitor, Ac-DEVD-CHO, did not protect HT-22 cells from Glu cytotoxicity, supporting a view that HT-22 cells do not express caspase 3.

4.5.4 Other possible factors

Oxidative stress in HT-22 cells induced by high concentration of extracellular Glu is characterized by the depletion in GSH and, consequently, the accumulation of

ROS. GSH consists of three amino acids, namely glycine, glutamate and cysteine. High concentrations of extracellular Glu inhibit the import of cystine, a precursor of cysteine, leading to depletion of intracellular cysteine and resulting in inhibition of GSH synthesis. One of the possible mechanisms by which neurons could be protected from oxidative stress is, therefore, to increase the intracellular levels of cysteine to enhance GSH synthesis. One of the L-glutamate transporters, excitatory amino acid transporter-3 (EAAT-3), localizes on neuronal cells while EAAT-1 and -2 predominantly localize on astrocytes (Rothstein et al., 1994). When EAAT-3 transports Glu into the neurons, it also brings cysteine into the cells (Chen and Swanson, 2003). Elevated extracellular Glu concentrations inhibit the function of EAAT-3. PLZ could protect cells by increasing the activity of EAAT-3 and/or the expression level of EAAT-3. To investigate this possibility of PLZ increasing EAAT-3 protein expression level, EAAT-3 protein levels can be compared in HT-22 cells untreated, Glu-treated, and PLZ plus Glu-treated. Western blotting for EAAT-3 using HT-22 cell extract was successful (data not shown). Therefore, investigating the expression levels should be possible by analyzing the Western blotting results. As for cysteine intracellular levels, measurement methods are well established (Davis and Maher, 1994). However, as discussed in earlier, the data presented here show that there is no neuroprotective effect of PLZ under H_2O_2 cytotoxicity, suggesting that an increase in GSH levels is likely to be a small part of the neuroprotection provided by PLZ.

Holt et al. (2004) reported that PLZ could interfere with various enzymes. Indeed, PLZ can bind to pyridoxal phosphate (PLP), which is a co-factor of many enzymes, and the binding of PLZ to PLP can lead to the depletion of PLP available for the activation of other enzymes. According to their report, 114 enzymes use PLP as cofactor and approximately 50 of these are expressed in humans. Half of the 50 enzymes expressed in humans are aminotransferases and a quarter are decarboxylases. Any of them could contribute to the neuroprotection from oxidative stress provided by PLZ. At this point in time, there is no supporting or opposing material for this hypothesis.

Oxidative stress induced cell death presents partial apoptotic features (Tan et al., 1998). These authors observed an ultrastructural damage of mitochondria membranes, and this damage could allow the leakage of ROS from the mitochondria to the cytosol. PLZ might be able to inhibit the membrane damage. To investigate this possibility, one can perform electron microscopic analysis of HT-22 cells treated with Glu or PLZ-Glu.

The data showing that PLZ did not protect neurons from H_2O_2 cytotoxicity implies that PLZ has little protective effect from damage induced by ROS. In other words, PLZ does not, or very weakly dose, reduce ROS levels. It is more likely that PLZ can suppress a *de novo* production of ROS. However, the NAP experimental results showed a smaller neuroprotective effect, suggesting that suppression of *de novo* synthesis of ROS by PLZ might involve another mechanism different from MAOI. As suggested earlier, monoamine uptake might

be up-regulated by oxidative stress and PLZ might inhibit the up-regulation of monoamine uptake.

4.6 PLZ utility for oxidative stress

The MAOI activity of PLZ probably plays an important role in preventing neuronal cell death induced by oxidative stress in that MAO is the main contributor to the synthesis of ROS during the post-ischemic period (Suzuki et al., 1995; Tadano et al., 1995). However, the results obtained with NAP treatment imply that MAOI may not be the sole component for the neuroprotective effects of PLZ from Glu induced cytotoxicity. A better understanding of the mechanisms by which PLZ provided neuroprotection against oxidative stress would be valuable for developing second-generation drugs from PLZ.

4.7 Conclusions and future directions

This thesis is the first study to characterize the GABAergic properties of HT-22 cells. HT-22 cells contain GABA and the GABA synthesizing enzymes, GAD_{65} and GAD_{67}, suggesting that HT-22 cells can synthesize GABA. The GABA metabolizing enzyme GABA-T was not detected by assaying for its activity or its mRNA and these findings indicate that HT-22 cells probably do not have the ability to degrade synthesized GABA. As future directions, the presence of GABA receptors, especially $GABA_A$ receptors on HT-22 cells should be investigated. Currently, the effect of GABA on neuronal cell viability under

oxidative stress has not been studied. If HT-22 cells have GABA receptors, they would provide an ideal model to study effects of GABA on neuronal cells without the excitotoxic effects of Glu because HT-22 cells lack Glu receptors (Maher and Davis, 1996).

In the second half of this thesis, the neuroprotective effect of PLZ and the possible mechanisms for this effect were reported. At 100 μM concentration, PLZ showed a significant and strong neuroprotective effect from 10 mM Glu toxicity. PEH, which lacks strong MAOI activity, did not protect neurons from Glu toxicity implying the importance of MAOI activity in neuroprotection provided by PLZ. However, the data from NAP experiments implied that the MAOI activity of PLZ may not be the sole component for its protective effects because NAP has MAOI activity similar to that of PLZ but showed much weaker neuroprotective effects.

The neuroprotective mechanisms provided by PLZ should be further studied. One direction would be to try using other metabolites of PLZ to study their effect on Glu-treated HT-22 cell viability. Specifically, some PLZ analogues, which do not have MAOI activity, might also demonstrate neuroprotective effects. Studying the effects of those analogue drugs would help us to understand the mechanism by which PLZ can protect neurons. Another direction is to further investigate possible pathways affected by PLZ treatment. For example, one could study whether or not other proteins involved in apoptotic pathways are affected by PLZ treatment, or whether PLZ helps maintain the cellular structure of mitochondria to prevent release of ROS from the mitochondria. Furthermore,

it would be important to investigate whether ROS-generating pathways are affected by PLZ. Oxidative stress may stimulate ROS synthesis by increasing monoamine uptake. PLZ might be inhibiting this uptake to effectively reduce the generation of ROS.

Experimental studies of new analogue drugs and HT-22 cells signal transduction pathways affected by PLZ administration would aid the development of new drugs for patients whose neurons are under attack from oxidative stress, thereby offering some relief to patients who have suffered strokes or who are suffering from Alzheimer's or Parkinson's diseases.

References

Alberts, B., D. Bray, J. Lewis, M. Raff, K. Roberts, and J.D. Watson. 1994. Molecular biology of the cell. 3rd edition:41-88.

Ashe, P.C., and M.D. Berry. 2003. Apoptotic signaling cascades. *Prog Neuropsychopharmacol Biol Psychiatry.* 27:199-214.

Baker, G.B., J.T. Wong, J.M. Yeung, and R.T. Coutts. 1991. Effects of the antidepressant phenelzine on brain levels of gamma-aminobutyric acid (GABA). *J Affect Disord.* 21:207-11.

Ballabriga, J., A. Pellise, and I. Ferrer. 1997. L-Deprenyl does not reduce brain damage in global forebrain ischemia in adult gerbils (Meriones ungiculatus). *J Neurol Sci.* 148:1-5.

Behl, C., M. Widmann, T. Trapp, and F. Holsboer. 1995. 17-beta estradiol protects neurons from oxidative stress-induced cell death in vitro. *Biochem Biophys Res Commun.* 216:473-82.

Bojes, H.K., K. Datta, J. Xu, A. Chin, P. Simonian, G. Nunez, and J.P. Kehrer. 1997. Bcl-xL overexpression attenuates glutathione depletion in FL5.12 cells following interleukin-3 withdrawal. *Biochem J.* 325 (Pt 2):315-9.

Bortner, C.D., N.B. Oldenburg, and J.A. Cidlowski. 1995. The role of DNA fragmentation in apoptosis. *Trends Cell Biol.* 5:21-26.

Braughler, J.M., and E.D. Hall. 1989. Central nervous system trauma and stroke. I. Biochemical considerations for oxygen radical formation and lipid peroxidation. *Free Radic Biol Med.* 6:289-301.

Buchan, A.M. 1990. Do NMDA antagonists protect against cerebral ischemia: are clinical trials warranted? *Cerebrovasc Brain Metab Rev.* 2:1-26.

Buchan, A.M., S.Z. Gertler, H. Li, D. Xue, Z.G. Huang, K.E. Chaundy, K. Barnes, and H.J. Lesiuk. 1994. A selective N-type Ca(2+)-channel blocker prevents CA1 injury 24 h following severe forebrain ischemia and reduces infarction following focal ischemia. *J Cereb Blood Flow Metab.* 14:903-10.

Chan, P.H., R. Kerlan, and R.A. Fishman. 1983. Reductions of gamma-aminobutyric acid and glutamate uptake and (Na+ + K+)-ATPase activity in brain slices and synaptosomes by arachidonic acid. *J Neurochem.* 40:309-16.

Chen, S.R., D.D. Dunigan, and M.B. Dickman. 2003. Bcl-2 family members inhibit oxidative stress-induced programmed cell death in Saccharomyces cerevisiae. *Free Radic Biol Med.* 34:1315-25.

Chen, Y., and R.A. Swanson. 2003. The glutamate transporters EAAT2 and EAAT3 mediate cysteine uptake in cortical neuron cultures. *J Neurochem.* 84:1332-9.

Cheung, R.T. 2003. The utility of melatonin in reducing cerebral damage resulting from ischemia and reperfusion. *J Pineal Res.* 34:153-60.

Colbourne, F., and D. Corbett. 1994. Delayed and prolonged post-ischemic hypothermia is neuroprotective in the gerbil. *Brain Res.* 654:265-72.

Dargusch, R., and D. Schubert. 2002. Specificity of resistance to oxidative stress. *J Neurochem.* 81:1394-400.

Davis, J.B., and P. Maher. 1994. Protein kinase C activation inhibits glutamate-induced cytotoxicity in a neuronal cell line. *Brain Res.* 652:169-73.

De Camilli, P., P.E. Miller, F. Navone, W.E. Theurkauf, and R.B. Vallee. 1984. Distribution of microtubule-associated protein 2 in the nervous system of the rat studied by immunofluorescence. *Neuroscience.* 11:817-46.

Dowden, J., C. Reid, P. Dooley, and D. Corbett. 1999. Diazepam-induced neuroprotection: dissociating the effects of hypothermia following global ischemia. *Brain Res.* 829:1-6.

Frederiksen, K., P.S. Jat, N. Valtz, D. Levy, and R. McKay. 1988. Immortalization of precursor cells from the mammalian CNS. *Neuron.* 1:439-48.

Gagliardi, R.J. 2000. Neuroprotection, excitotoxicity and NMDA antagonists. *Arq Neuropsiquiatr.* 58:583-8.

Gill, R., A.C. Foster, and G.N. Woodruff. 1988. MK-801 is neuroprotective in gerbils when administered during the post-ischaemic period. *Neuroscience.* 25:847-55.

Goldberg, M.P., and D.W. Choi. 1993. Combined oxygen and glucose deprivation in cortical cell culture: calcium-dependent and calcium-independent mechanisms of neuronal injury. *J Neurosci.* 13:3510-24.

Green, P.S., S.H. Yang, K.R. Nilsson, A.S. Kumar, D.F. Covey, and J.W. Simpkins. 2001. The nonfeminizing enantiomer of 17beta-estradiol exerts protective effects in neuronal cultures and a rat model of cerebral ischemia. *Endocrinology.* 142:400-6.

Gursoy, E., A. Cardounel, and M. Kalimi. 2001. The environmental estrogenic compound bisphenol A exerts estrogenic effects on mouse hippocampal (HT-22) cells: neuroprotection against glutamate and amyloid beta protein toxicity. *Neurochem Int.* 38:181-86.

Hall, E.D., T.J. Fleck, and J.A. Oostveen. 1998. Comparative neuroprotective properties of the benzodiazepine receptor full agonist diazepam and the partial agonist PNU-101017 in the gerbil forebrain ischemia model. *Brain Res.* 798:325-9.

Hansen, A.J., J. Hounsgaard, and H. Jahnsen. 1982. Anoxia increases potassium conductance in hippocampal nerve cells. *Acta Physiol Scand.* 115:301-10.

Hasegawa, Y., and B. Bonavida. 1989. Calcium-independent pathway of tumor necrosis factor-mediated lysis of target cells. *J Immunol.* 142:2670-6.

Henderson, V.W., M. Cunningham, N. Valtz, and M.R.D. G. 1989. *Soc. Neurosci. Abstr.* 15:1093.

Hengartner, M.O., and H.R. Horvitz. 1994a. Activation of C. elegans cell death protein CED-9 by an amino-acid substitution in a domain conserved in Bcl-2. *Nature.* 369:318-20.

Hengartner, M.O., and H.R. Horvitz. 1994b. C. elegans cell survival gene ced-9 encodes a functional homolog of the mammalian proto-oncogene bcl-2. *Cell.* 76:665-76.

Holt, A., M.D. Berry, and A.A. Boulton. 2004. On the binding of monoamine oxidase inhibitors to some sites distinct from the MAO active site, and effects thereby elicited. *Neurotoxicology.* 25:251-66.

Inglefield, J.R., J.M. Perry, and R.D. Schwartz. 1995. Postischemic inhibition of GABA reuptake by tiagabine slows neuronal death in the gerbil hippocampus. *Hippocampus*. 5:460-8.

Jacobsson, S.O., and C.J. Fowler. 1999. Dopamine and glutamate neurotoxicity in cultured chick telencephali cells: effects of NMDA antagonists, antioxidants and MAO inhibitors. *Neurochem Int*. 34:49-62.

Jiang, C., S. Agulian, and G.G. Haddad. 1992. Cl^- and Na^+ homeostasis during anoxia in rat hypoglossal neurons: intracellular and extracellular in vitro studies. *J Physiol*. 448:697-708.

Johansen, F.F. 1993. Interneurons in rat hippocampus after cerebral ischemia. Morphometric, functional, and therapeutic investigations. *Acta Neurol Scand Suppl*. 150:1-32.

Johansen, F.F., and N.H. Diemer. 1991. Enhancement of GABA neurotransmission after cerebral ischemia in the rat reduces loss of hippocampal CA1 pyramidal cells. *Acta Neurol Scand*. 84:1-6.

Kayser, A., D.S. Robinson, K. Yingling, D.B. Howard, J. Corcella, and D. Laux. 1988. The influence of panic attacks on response to phenelzine and amitriptyline in depressed outpatients. *J Clin Psychopharmacol*. 8:246-53.

Kerr, J.F., A.H. Wyllie, and A.R. Currie. 1972. Apoptosis: a basic biological phenomenon with wide-ranging implications in tissue kinetics. *Br J Cancer*. 26:239-57.

Kimura, M., K. Sawada, T. Miyagawa, M. Kuwada, K. Katayama, and Y. Nishizawa. 1998. Role of glutamate receptors and voltage-dependent calcium and sodium channels in the extracellular glutamate/aspartate accumulation and subsequent neuronal injury induced by oxygen/glucose deprivation in cultured hippocampal neurons. *J Pharmacol Exp Ther*. 285:178-85.

Klein, J.A., and S.L. Ackerman. 2003. Oxidative stress, cell cycle, and neurodegeneration. *J Clin Invest*. 111:785-93.

Kumar, S. 1995. ICE-like proteases in apoptosis. *Trends Biochem Sci*. 20:198-202.

Langston, J.W., I. Irwin, E.B. Langston, and L.S. Forno. 1984. Pargyline prevents MPTP-induced parkinsonism in primates. *Science*. 225:1480-2.

Lev, N., E. Melamed, and D. Offen. 2003. Apoptosis and Parkinson's disease. *Prog Neuropsychopharmacol Biol Psychiatry*. 27:245-50.

Li, H., and A.M. Buchan. 1993. Treatment with an AMPA antagonist 12 hours following severe normothermic forebrain ischemia prevents CA1 neuronal injury. *J Cereb Blood Flow Metab*. 13:933-9.

Liebowitz, M.R., F.M. Quitkin, J.W. Stewart, P.J. McGrath, W.M. Harrison, J.S. Markowitz, J.G. Rabkin, E. Tricamo, D.M. Goetz, and D.F. Klein. 1988. Antidepressant specificity in atypical depression. *Arch Gen Psychiatry*. 45:129-37.

Lipton, P. 1999. Ischemic cell death in brain neurons. *Physiol Rev*. 79:1431-568.

Liu, Q.A., and M.O. Hengartner. 1999. The molecular mechanism of programmed cell death in C. elegans. *Ann N Y Acad Sci*. 887:92-104.

Lyden, P.D., and L. Lonzo. 1994. Combination therapy protects ischemic brain in rats. A glutamate antagonist plus a gamma-aminobutyric acid agonist. *Stroke*. 25:189-96.

Maher, P., and J.B. Davis. 1996. The role of monoamine metabolism in oxidative glutamate toxicity. *J Neurosci*. 16:6394-401.

Martin, L.J., N.A. Al-Abdulla, A.M. Brambrink, J.R. Kirsch, F.E. Sieber, and C. Portera-Cailliau. 1998. Neurodegeneration in excitotoxicity, global cerebral ischemia, and target deprivation: A perspective on the contributions of apoptosis and necrosis. *Brain Res Bull*. 46:281-309.

McKenna, K.F., G.B. Baker, and R.T. Coutts. 1991. N2-acetylphenelzine: effects, on rat brain GABA, alanine and biogenic amines. *Naunyn Schmiedebergs Arch Pharmacol*. 343:478-82.

McKenna, K.F., G.B. Baker, R.T. Coutts, and A.J. Greenshaw. 1992. Chronic administration of the antidepressant-antipanic drug phenelzine and its N-acetylated analogue: effects on monoamine oxidase, biogenic amines, and alpha 2-adrenoreceptor function. *J Pharm Sci*. 81:832-5.

Medina-Kauwe, L.K., N.J. Tillakaratne, J.Y. Wu, and A.J. Tobin. 1994. A rat brain cDNA encodes enzymatically active GABA transaminase and provides a molecular probe for GABA-catabolizing cells. *J Neurochem*. 62:1267-75.

Merry, D.E., and S.J. Korsmeyer. 1997. Bcl-2 gene family in the nervous system. *Annu Rev Neurosci*. 20:245-67.

Moody, A.R., R.E. Murphy, P.S. Morgan, A.L. Martel, G.S. Delay, S. Allder, S.T. MacSweeney, W.G. Tennant, J. Gladman, J. Lowe, and B.J. Hunt. 2003. Characterization of complicated carotid plaque with magnetic resonance direct thrombus imaging in patients with cerebral ischemia. *Circulation*. 107:3047-52.

Mozayani, A., R.T. Coutts, T.J. Danielson, and G.B. Baker. 1988. Metabolic acetylation of phenelzine in rats. *Res Commun Chem Pathol Pharmacol*. 62:397-406.

Murphy, T.H., M. Miyamoto, A. Sastre, R.L. Schnaar, and J.T. Coyle. 1989. Glutamate toxicity in a neuronal cell line involves inhibition of cystine transport leading to oxidative stress. *Neuron*. 2:1547-58.

Neumann, C., Boubakari, R. Grunert, and P.J. Bednarski. 2003. Nicotinamide adenine dinucleotide phosphate-regenerating system coupled to a glutathione-reductase microtiter method for determination of total glutathione concentrations in adherent growing cancer cell lines. *Anal Biochem*. 320:170-8.

Nguyen, M., P.E. Branton, P.A. Walton, Z.N. Oltvai, S.J. Korsmeyer, and G.C. Shore. 1994. Role of membrane anchor domain of Bcl-2 in suppression of apoptosis caused by E1B-defective adenovirus. *J Biol Chem*. 269:16521-4.

Nguyen, M., D.G. Millar, V.W. Yong, S.J. Korsmeyer, and G.C. Shore. 1993. Targeting of Bcl-2 to the mitochondrial outer membrane by a COOH-terminal signal anchor sequence. *J Biol Chem*. 268:25265-8.

O'Neill, M.J., L. Bogaert, C.A. Hicks, A. Bond, M.A. Ward, G. Ebinger, P.L. Ornstein, Y. Michotte, and D. Lodge. 2000. LY377770, a novel iGlu5

kainate receptor antagonist with neuroprotective effects in global and focal cerebral ischaemia. *Neuropharmacology*. 39:1575-88.
Ottilie, S., Y. Wang, S. Banks, J. Chang, N.J. Vigna, S. Weeks, R.C. Armstrong, L.C. Fritz, and T. Oltersdorf. 1997. Mutational analysis of the interacting cell death regulators CED-9 and CED-4. *Cell Death Differ.* 4:526-33.
Parent, M.B., S. Master, S. Kashlub, and G.B. Baker. 2002. Effects of the antidepressant/antipanic drug phenelzine and its putative metabolite phenylethylidenehydrazine on extracellular gamma-aminobutyric acid levels in the striatum. *Biochem Pharmacol.* 63:57-64.
Paslawski, T., E. Knaus, N. Iqbal, R.T. Coutts, and G.B. Baker. 2001. ß-Phenelethylidenehydrazine, a novel inhibitor of GABA transminase. *Drug Devel. Res.* 54:35-39.
Phillis, J.W. 1995. CI-966, a GABA uptake inhibitor, antagonizes ischemia-induced neuronal degeneration in the gerbil. Gen Pharmacol. 26:1061-4.
Popov, N., and H. Matthies. 1969. Some effects of monoamine oxidase inhibitors on the metabolism of gamma-aminobutyric acid in rat brain. J Neurochem. 16:899-907.
Priault, M., N. Camougrand, B. Chaudhuri, and S. Manon. 1999. Role of the C-terminal domain of Bax and Bcl-XL in their localization and function in yeast cells. *FEBS Lett.* 443:225-8.
Prokai, L., S.M. Oon, K. Prokai-Tatrai, K.A. Abboud, and J.W. Simpkins. 2001. Synthesis and biological evaluation of 17beta-alkoxyestra-1,3, 5(10)-trienes as potential neuroprotectants against oxidative stress. *J Med Chem.* 44:110-4.
Roberts, J.C., and D.J. Francetic. 1993. The importance of sample preparation and storage in glutathione analysis. *Anal Biochem.* 211:183-7.
Rothstein, J.D., L. Martin, A.I. Levey, M. Dykes-Hoberg, L. Jin, D. Wu, N. Nash, and R.W. Kuncl. 1994. Localization of neuronal and glial glutamate transporters. *Neuron.* 13:713-25.
Sagara, Y., R. Dargusch, D. Chambers, J. Davis, D. Schubert, and P. Maher. 1998. Cellular mechanisms of resistance to chronic oxidative stress. *Free Radic Biol Med.* 24:1375-89.
Sagara, Y., S. Hendler, S. Khoh-Reiter, G. Gillenwater, D. Carlo, D. Schubert, and J. Chang. 1999. Propofol hemisuccinate protects neuronal cells from oxidative injury. *J Neurochem.* 73:2524-30.
Sah, R., F. Galeffi, R. Ahrens, G. Jordan, and R.D. Schwartz-Bloom. 2002. Modulation of the GABA(A)-gated chloride channel by reactive oxygen species. *J Neurochem.* 80:383-91.
Saransaari, P., and S.S. Oja. 1998. Release of endogenous glutamate, aspartate, GABA, and taurine from hippocampal slices from adult and developing mice under cell-damaging conditions. *Neurochem Res.* 23:563-70.
Sato, H., M. Tamba, T. Ishii, and S. Bannai. 1999. Cloning and expression of a plasma membrane cystine/glutamate exchange transporter composed of two distinct proteins. *J Biol Chem.* 274:11455-8.

Schroder, M.L., J.P. Muizelaar, A.J. Kuta, and S.C. Choi. 1996. Thresholds for cerebral ischemia after severe head injury: relationship with late CT findings and outcome. *J Neurotrauma*. 13:17-23.

Schwartz, R.D., R.A. Huff, X. Yu, M.L. Carter, and M. Bishop. 1994. Postischemic diazepam is neuroprotective in the gerbil hippocampus. *Brain Res*. 647:153-60.

Schwartz-Bloom, R.D., and R. Sah. 2001. gamma-Aminobutyric acid(A) neurotransmission and cerebral ischemia. *J Neurochem*. 77:353-71.

Serrano, J.S., F.J. Minano, M. Sancibrian, and J.A. Duran. 1985. Involvement of bicuculline-insensitive receptors in the hypothermic effect of GABA and its agonists. *Gen Pharmacol*. 16:505-8.

Sheardown, M.J., P.D. Suzdak, and L. Nordholm. 1993. AMPA, but not NMDA, receptor antagonism is neuroprotective in gerbil global ischaemia, even when delayed 24 h. *Eur J Pharmacol*. 236:347-53.

Silver, I.A., and M. Erecinska. 1990. Intracellular and extracellular changes of [Ca2+] in hypoxia and ischemia in rat brain in vivo. *J Gen Physiol*. 95:837-66.

Singer, T.P., and R.R. Ramsay. 1995. Flauoprotein structure and mechanism 2. Monoamine oxidases: old friends hold many surprises. *Faseb J*. 9:605-10.

Speiser, Z., A. Mayk, S. Eliash, and S. Cohen. 1999. Studies with rasagiline, a MAO-B inhibitor, in experimental focal ischemia in the rat. *J Neural Transm*. 106:593-606.

Strausberg, R.L., E.A. Feingold, L.H. Grouse, J.G. Derge, R.D. Klausner, F.S. Collins, L. Wagner, C.M. Shenmen, G.D. Schuler, S.F. Altschul, B. Zeeberg, K.H. Buetow, C.F. Schaefer, N.K. Bhat, R.F. Hopkins, H. Jordan, T. Moore, S.I. Max, J. Wang, F. Hsieh, L. Diatchenko, K. Marusina, A.A. Farmer, G.M. Rubin, L. Hong, M. Stapleton, M.B. Soares, M.F. Bonaldo, T.L. Casavant, T.E. Scheetz, M.J. Brownstein, T.B. Usdin, S. Toshiyuki, P. Carninci, C. Prange, S.S. Raha, N.A. Loquellano, G.J. Peters, R.D. Abramson, S.J. Mullahy, S.A. Bosak, P.J. McEwan, K.J. McKernan, J.A. Malek, P.H. Gunaratne, S. Richards, K.C. Worley, S. Hale, A.M. Garcia, L.J. Gay, S.W. Hulyk, D.K. Villalon, D.M. Muzny, E.J. Sodergren, X. Lu, R.A. Gibbs, J. Fahey, E. Helton, M. Ketteman, A. Madan, S. Rodrigues, A. Sanchez, M. Whiting, A.C. Young, Y. Shevchenko, G.G. Bouffard, R.W. Blakesley, J.W. Touchman, E.D. Green, M.C. Dickson, A.C. Rodriguez, J. Grimwood, J. Schmutz, R.M. Myers, Y.S. Butterfield, M.I. Krzywinski, U. Skalska, D.E. Smailus, A. Schnerch, J.E. Schein, S.J. Jones, and M.A. Marra. 2002. Generation and initial analysis of more than 15,000 full-length human and mouse cDNA sequences. *Proc Natl Acad Sci U S A*. 99:16899-903.

Stys, P.K. 1998. Anoxic and ischemic injury of myelinated axons in CNS white matter: from mechanistic concepts to therapeutics. *J Cereb Blood Flow Metab*. 18:2-25.

Sulston, J.E. 2003. C. elegans: the cell lineage and beyond. *Biosci Rep*. 23:49-66.

Suzuki, T., N. Akaike, K. Ueno, Y. Tanaka, and N. Himori. 1995. MAO inhibitors, clorgyline and lazabemide, prevent hydroxyl radical generation caused by brain ischemia/reperfusion in mice. *Pharmacology*. 50:357-62.

Tadano, T., A. Yonezawa, K. Oyama, K. Kisara, Y. Arai, M. Togashi, and H. Kinemuchi. 1995. Effects of transient global ischemia and a monoamine oxidase inhibitor ifenprodil on rat brain monoamine metabolism. *Prog Brain Res*. 106:173-80.

Tan, S., M. Wood, and P. Maher. 1998. Oxidative stress induces a form of programmed cell death with characteristics of both apoptosis and necrosis in neuronal cells. *J Neurochem*. 71:95-105.

Tanay, V.A., M.B. Parent, J.T. Wong, T. Paslawski, I.L. Martin, and G.B. Baker. 2001. Effects of the antidepressant/antipanic drug phenelzine on alanine and alanine transaminase in rat brain. Cell Mol Neurobiol. 21:325-39.

Teitze, F. 1969. Enzymatic method for quantitative determination of nanogram amounts of total oxidized glutathione: Applications to mammalian blood and other tissues. *Anal. Biochem.* 27:502-522.

Thioudellet, C., T. Oster, P. Leroy, A. Nicolas, and M. Wellman. 1995. Influence of sample preparation on cellular glutathione recovery from adherent cells in culture. *Cell Biol Toxicol*. 11:103-11.

Todd, K.G., and G.B. Baker. 1995. GABA-elevating effects of the antidepressant/antipanic drug phenelzine in brain: effects of pretreatment with tranylcypromine, (-)-deprenyl and clorgyline. *J Affect Disord*. 35:125-9.

Todd, K.G., A.I. Banigesh, G.B. Baker, R.T. Coutts, and A. Shuaib. 1999. Phenylethylidenehydrazine, a novel GABA-T inhibitor has neuroprotective actions in transient global ischemia. *J. Neurochem.* 73.

Tremblay, R., B. Chakravarthy, K. Hewitt, J. Tauskela, P. Morley, T. Atkinson, and J.P. Durkin. 2000. Transient NMDA receptor inactivation provides long-term protection to cultured cortical neurons from a variety of death signals. *J Neurosci*. 20:7183-92.

Vanella, A., C. Di Giacomo, V. Sorrenti, A. Russo, C. Castorina, A. Campisi, M. Renis, and J.R. Perez-Polo. 1993. Free radical scavenger depletion in post-ischemic reperfusion brain damage. *Neurochem Res*. 18:1337-40.

Weyler, W., Y.P. Hsu, and X.O. Breakefield. 1990. Biochemistry and genetics of monoamine oxidase. *Pharmacol Ther*. 47:391-417.

Williams, A.J., and F.C. Tortella. 2002. Neuroprotective effects of the sodium channel blocker RS100642 and attenuation of ischemia-induced brain seizures in the rat. *Brain Res*. 932:45-55.

Wu, D., H.D. Wallen, N. Inohara, and G. Nunez. 1997. Interaction and regulation of the Caenorhabditis elegans death protease CED-3 by CED-4 and CED-9. *J Biol Chem*. 272:21449-54.

Xue, D., S. Shaham, and H.R. Horvitz. 1996. The Caenorhabditis elegans cell-death protein CED-3 is a cysteine protease with substrate specificities similar to those of the human CPP32 protease. *Genes Dev*. 10:1073-83.

Yu, P.H., and K.F. Tipton. 1989. Deuterium isotope effect of phenelzine on the inhibition of rat liver mitochondrial monoamine oxidase activity. Biochem Pharmacol. 38:4245-51.

Zou, H., W.J. Henzel, X. Liu, A. Lutschg, and X. Wang. 1997. Apaf-1, a human protein homologous to C. elegans CED-4, participates in cytochrome c-dependent activation of caspase-3. *Cell*. 90:405-13.